

United Kingdom Atomic Energy Authority

HARWELL

U.K. Nuclear Data Progress Report

January – December 1988

Editors: M R Sené and J A Cookson

Nuclear Physics and Instrumentation Division
Harwell Laboratory, Oxfordshire OX11 0RA

March 1990

© - UNITED KINGDOM ATOMIC ENERGY AUTHORITY - 1990
Enquiries about copyright and reproduction should be addressed to the Publications
Office, Harwell Laboratory, Oxfordshire, OX11 0RA, England

UNCLASSIFIED

UKNDC(89)P116
NEANDC(E)302
INDC(UK)-044/LN

U.K. NUCLEAR DATA PROGRESS REPORT

January - December 1988

Editors: M. R. Sené and J. A. Cookson

Nuclear Physics and
Instrumentation Division
Harwell Laboratory
Oxfordshire
OX11 0RA

PREFACE

This report, summarising nuclear data research in the United Kingdom in 1988, has been prepared on behalf of the Nuclear Data Committee (UKNDC).

Contributions have been received this year from Harwell Laboratory, the UK Chemical Nuclear Data Committee (UKCND), the National Physical Laboratory and the University of Oxford. The reduction over the past few years of the number of such contributions to this report is a reflection of the reduced activity, due primarily to reduced funding, in the field of nuclear data. However, the work described in this report includes contributions from and/or collaboration with a much larger number of institutions, namely: AEE Winfrith, DNPDE Dounreay, JET, AWE, Aldermaston, Imperial College Reactor Centre, Queen Mary College London, University of Manchester, University of Milan Italy, KfK Karlsruhe, West Germany, ECN Petten, The Netherlands, Ohio University, USA and the Institute for Atomic Energy Beijing, China.

The editors would like to thank all those who contributed to this report for their prompt response to our request.

CONTENTS

	<u>Page No.</u>
1. <u>NUCLEAR PHYSICS DIVISION, HARWELL LABORATORY</u>	
1.1 Iron capture cross-section measurements.	1
1.2 Total cross-section measurements.	5
1.3 Fission chambers for the intercomparison of fast neutron flux density measurements.	8
1.4 Resonant neutron capture gamma-ray spectroscopy in the structural materials.	9
1.5 The use of neutron intensity calibrated ^9Be (α, n) sources as 4438 keV gamma-ray reference standards.	12
1.6 The absolute determination of the response function of the Harwell Total Energy detector to 6.13 MeV gamma-rays.	18
1.7 The potential for making accurate absolute measurements of the HELIOS neutron spectrum below 200 keV using a ^{10}B sample and a pair of high purity germanium gamma-ray spectrometers.	28
1.8 Evaluation of cross-sections for the Joint Evaluated File.	32
1.9 FISPIN on the Harwell computer.	37
1.10 Fusion reactor activation calculations.	37
1.11 Measurements of gamma-ray excitation functions in support of JET gamma-ray diagnostics.	43
2. <u>CHEMICAL NUCLEAR DATA</u>	
2.1 Introduction.	51
2.2 Measurements.	52
2.2.1 Yield of tritium in ternary fission	52
2.2.2 Absolute fission yields of selected fission products.	53
2.2.3 Measurements of alpha in PFR.	53
2.2.4 Measurement of radionuclide decay data.	54
2.2.5 Measurement and evaluations of half-lives and gamma-ray emission probabilities.	55
2.3 CNC data library sub-committee.	55
2.3.1 Data library development.	56
2.3.2 Joint evaluated file, JEF.	61

3. DIVISION OF RADIATION SCIENCE AND ACOUSTICS,
NATIONAL PHYSICAL LABORATORY

- 3.1 International intercomparisons 3.1.1
Radioactivity measurements.
- 3.2 Neutron cross-sections.
- 3.3 Decay data.
- 3.4 Evaluations.

4. NUCLEAR PHYSICS LABORATORY, UNIVERSITY OF OXFORD

- 4.1 The unification of the nuclear optical potential.
- 4.2 Multistep analysis of neutron and proton induced reactions below 20 MeV.
- 4.3 Neutron emission cross-sections on ^{184}W at 11.5 MeV and 26.0 MeV and the neutron-nucleus scattering mechanisms.
- 4.4 Work on nuclear model codes.
 - 4.4.1 International nuclear model code intercomparison.
 - 4.4.2 Weisskopf-Ewing and Hauser-Feshbach international nuclear model code intercomparison.
- 4.5 Nucleon momentum distributions.
- 4.6 Nucleon-alpha reactions in nuclei.
- 4.7 Recent publications.

1. NUCLEAR PHYSICS DIVISION, HARWELL LABORATORY

(Division Head: Dr. A. T. G. Ferguson)

1.1 Iron capture cross-section measurements (D. B. Gayther, J. E. Jolly and R. B. Thom (Tessella Support Services Ltd.))

Previous progress reports (UKNDC(87)P115, p.3, UKNDC(86)P113, p.6) have described time-of-flight measurements of the capture cross-section of iron which have been made on HELIOS with a gamma-ray detector using the pulse amplitude weighting technique. The work is in support of the Task Force which was set up by the NEANDC to resolve the large discrepancies between capture and transmission measurements of the 1.15 keV resonance parameters.

Two series of measurements have been made. In the first, relative capture yields from a 2 mm thick natural iron sample were obtained. These data allow the 1.15 keV parameters to be determined relative to the parameters of other resonances in iron. In the second series a thin laminated sample of iron and gold was used, allowing absolute resonance parameters to be obtained by normalising the capture yield at the "saturated resonance" in gold at 4.9 eV.

Most of the discrepancy between capture and transmission data for the 1.15 keV resonance arises from capture measurements using the amplitude weighting technique. In this technique, the weighting function is derived from a series of pulse amplitude spectra for different gamma-ray energies. In the absence of convenient monoenergetic gamma-ray sources above 2.6 MeV, it is usual to calculate the spectra with a Monte Carlo code. The validity of the weighting function therefore depends on the ability of the code to model a capture event in the detector. Until recently, the calculated spectra only poorly represented

the observed spectra for the higher energy gamma-rays. Much of the present discrepancy probably stems from this lack of agreement, the capture gamma-ray spectrum from the 1.15 keV resonance being particularly "hard".

Perey et al⁽¹⁾ have shown that when a comprehensive code such as EGS4⁽²⁾ is used to calculate the detector gamma-ray response, good agreement with the experimental response is obtained at all energies provided that proper account is taken of the effect of all the materials in the vicinity of the source and the detector. The earlier disagreement arose mostly from inadequate treatment of electron tracking in local materials. In another contribution to this progress report Croft et al show that the response of the present detector to 6.13 MeV gamma-rays can be well reproduced by EGS4.

Tests of the sensitivity of resonance parameters derived by the weighting technique to the actual shape of the weighting function have been made. These indicate that, at the level of agreement between observed and calculated gamma-ray responses obtained with EGS4, the uncertainty introduced in the parameters from the application of the calculated weighting function should not be greater than about 3%. A weighting function for energies up to 12 MeV has been generated with the EGS4 code for each of the capture sample geometries used in the present measurements and the results obtained with these functions are now considered.

2mm iron sample

Time-of-flight measurements have been made of the capture yield from a 2 mm thick sample of natural iron in the energy range 190 eV to 120 keV. The

-
- (1) F. G. Perey, J. O. Johnson, T. A. Gabriel, R. L. Macklin, R. R. Winters, J. H. Todd and N. W. Hill, Proc. Conf. Nucl. Data for Science and Technology, p.379, Saikon Publ. Co., Tokyo (1988).
 - (2) EGS4, RSIC Computer Code Collection -331, Oak Ridge National Laboratory.

shape of the incident neutron spectrum was determined by replacing the iron sample with a ^{10}B sample. The yield obtained is not absolute, but the parameters of the 1.15 keV resonance are determined relative to those of the 22.8 keV resonance in ^{56}Fe which has a much "softer" capture gamma-ray spectrum than that from the 1.15 keV resonance. This difference in spectra led Weston and Todd⁽¹⁾ to compare measured capture areas ($g\Gamma_n\Gamma_\gamma/\Gamma$) of the two resonances as a means of testing the validity of their weighting function. The ratio of the areas obtained using the area analysis code CAREA⁽²⁾ are compared below with the values reported by Weston and Todd.

Table 1.1 Ratio of capture area 22.8 keV/1.15 keV

Measurement	Ratio
ORNL ⁽¹⁾ (transmission)	2.83±0.16
Weston and Todd ⁽¹⁾ (capture)	2.91±0.17
Present (capture)	2.55±0.16

Although the present ratio is 10% lower than the transmission value, the difference is not unreasonable in view of the uncertainties. Analysis with the original Harwell weighting function⁽³⁾ gives a ratio of 2.39±0.16. It is apparent that the use of the weighting function based on EGS4 calculations which properly model the experimental geometry gives somewhat better agreement with the transmission value.

-
- (1) L. W. Weston and J. H. Todd, Nuclear Data for Basic and Applied Science, Vol. 1, p.583, Gordon and Breach, New York (1986).
 (2) M. C. Moxon, private communication.
 (3) D. B. Gayther and R. B. Thom, Report ANL-83-4, p.205 (1983).

Laminated sample of iron and gold

Time-of-flight measurements have been made on the 42 m flight path in the energy range 2.4 eV to 110 keV using a laminated sample of iron and gold sheet in the form, 0.3 mm Fe - 25 μ m Au - 0.3 mm Fe. This arrangement allows absolute iron capture cross-sections to be obtained by normalizing the observed capture yield by the "saturated resonance" method at the 4.9 eV resonance in gold. This method relies on the fact that in a resonance with a large peak cross-section, and in which the dominant interaction is neutron capture, the capture yield (capture events per incident neutron) will approach unity near the peak, even when the sample is relatively thin. Calculation of the exact yield for the purpose of normalization is thus insensitive to the precise value of the resonance parameters.

The shape of the incident neutron spectrum was determined by replacing the iron/gold sample with a ^{10}B sample. The capture area of the ^{56}Fe 1.15 keV resonance derived from the measured capture yield with the code CAREA⁽¹⁾ is shown below.

Table 1.2 Capture area of 1.15 keV resonance

Measurement	$g\Gamma_n\Gamma_\gamma/\Gamma$ (meV)
ORNL (transmission) ⁽¹⁾	55.7 \pm 0.7
Harwell (transmission) ⁽²⁾	57.8 \pm 0.7
Present (capture)	59.5 \pm 3.0

(1) F. G. Perey, Nuclear Data for Basic and Applied Science, Vol. 2, p.1523, Gordon and Breach, New York (1986).

(2) G. D. James and M. C. Moxon, private communication.

Analysis of the present measurements with the original Harwell weighting function⁽¹⁾ gives an area of 65.0 ± 3.0 meV.

The results obtained from the two sets of measurements reported here are in better agreement with accurate transmission data than those obtained from our previous analysis based on a less satisfactory weighting function. It is intended to improve the resonance analysis of these data by using a comprehensive shape analysis code.

1.2 Total cross-section measurements (M. C. Moxon, D. S. Bond and J. B. Brisland)

Measurements of the neutron transmission of four thick samples of sodium have been carried out on the 150 m flight path on the fast neutron target of HELIOS. These measurements are in response to the request of the European Fast Reactor Project for an accurate value of the total cross-section of sodium in the energy regions around the minima at 300 and 500 keV for deep penetration studies.

Figure 1.1 shows the measured total cross-section as a function of time-of-flight channel number (i.e. from 1 MeV to 150 keV). These data, together with some data from Oak Ridge National Laboratory⁽²⁾ on a thinner sample, have been analysed with the program REFIT to obtain the resonance parameters and the effective scattering radii in the neutron energy region below 480 keV. The initial values of the nuclear parameters obtained from fits in the neutron energy region from 30 to 480 keV are given in Table 1.3. These

(1) D. B. Gayther and R. B. Thom, Report ANL-83-4, p.205 (1983).

(2) D. C. Larson, J. A. Harvey and N. W. Hill, ORNL/TM-5614 (1976).

Table 1.3 Nuclear parameters obtained from fits to data over the neutron energy range 30 to 480 keV

Spin		E_n (keV)	Γ_n (eV)	Γ_γ (eV)
J	L			
[1]	[1]	35.2955±0.0012	26.28± 0.19	1.90
2	1	53.1531±0.0028	1109.1 ± 3.0	0.785
[1]	[1]	117.3508±0.0009	24.16± 0.48	4.23
[0]	[1]	143.0777±0.0042	15.70± 1.44	7.1
[0]	[2]	189.7610±0.0120	17.55± 2.0	9.3
1	[1]	200.9623±0.0059	4124.7 ± 17.6	2.94
0	[1]	213.6053±0.0420	20729. ±138.0	4.64
J≤3	[2]	236.5761±0.0031	40.18± 1.07	1.0
2	[1]	239.1193±0.0060	5633.6 ± 12.4	1.20
0	[2]	242.7992±0.020	405.7 ± 18.1	1.0
1	0	242.9738±0.0030	345.28± 4.4	4.61
2	0	298.6500	2148.9 ± 4.7	1.14
J≥3	[1]	299.5347±0.0041	58.01± 1.45	1.0
[0]	[2]	305.3393±0.015	67.11± 6.0	9.7
1	1	394.9138±0.0233	26282. ± 57.4	9.89
0	1	431.8530±0.0300	6976.2 ± 88.5	5.29
2	1	449.6872±0.0101	6738.9 ± 17.3	4.2
Nuclear Radius $a_{\text{Jeff}} = a_0(1 - R_J^\infty)$ $a_0 = 3.839 \text{ fm}$				
J	L	R_∞		
1	0	-0.3647±0.0034		
2	0	-0.3524±0.0020		
0	1	1.6148±0.038		
1	1	0.5770±0.0102		
2	1	-0.7414±0.0094		
3	1	0.0		
0	2	0.0		
3	2	0.0		
4	2	0.0		

[] assumed spin and l values that fit the data, the others are fixed by the data. Parameters with no errors are fixed at given values.

Note These parameters can only be used to calculate the total neutron cross-section of sodium from 30 keV to 480 keV.

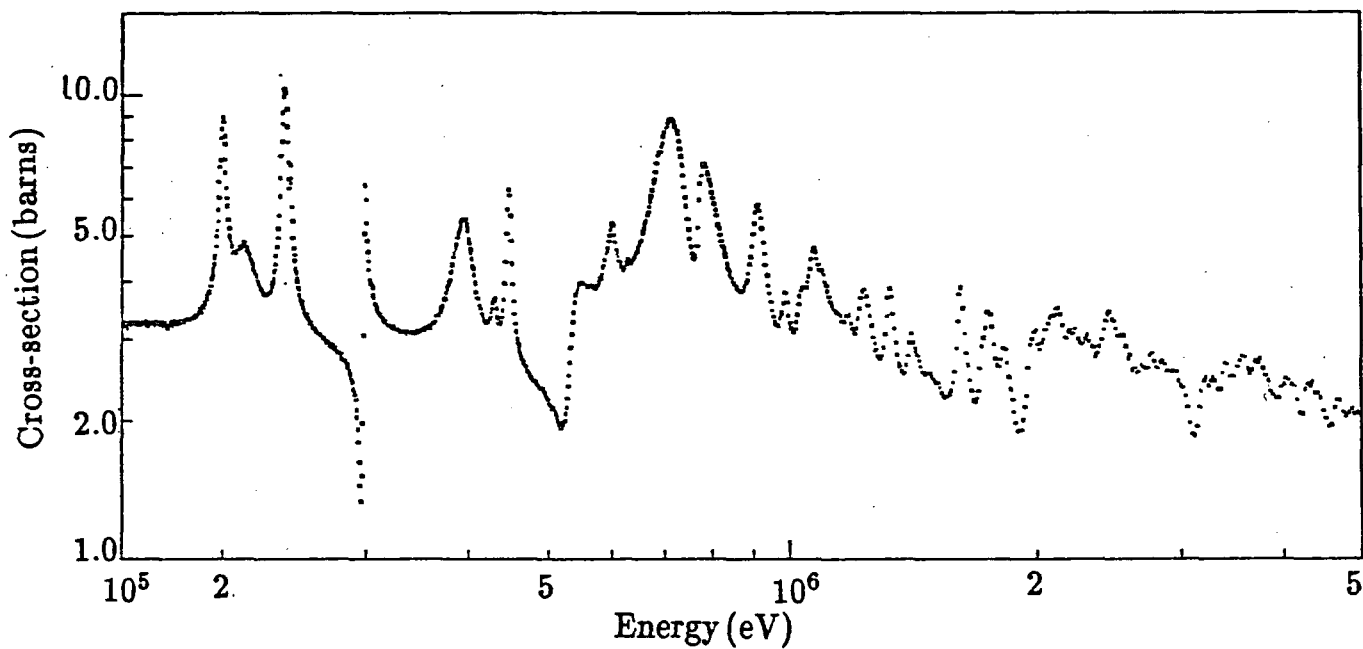


Figure 1.1 The measured total cross-section of sodium.

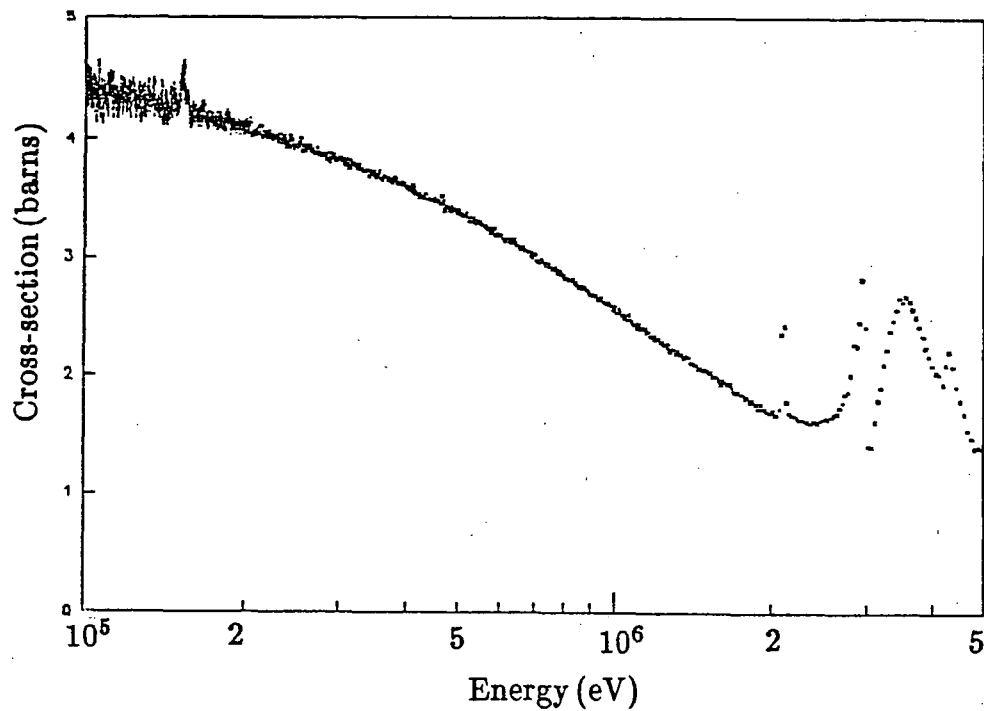


Figure 1.2 The measured total cross-section of carbon.

give an accurate total cross-section in the region from 30 to 480 keV only when used with the Reich-Moore multi-level formalism.

The final value of the total cross-section in the energy region between 150 keV and 480 keV has been measured to an accuracy of a few tens of millibarns and can be reproduced by the parameters given in Table 1.3.

As the analysis program REFIT has only the facility to calculate elastic and capture cross-sections, it cannot be used to analyse the data above the inelastic level at 480 keV. The analysis of the data above 480 keV will have to await the modification of the program to include the calculation of the inelastic cross-section.

To check the accuracy of the sodium data, measurements were also carried out on a thick carbon sample. Figure 1.2 shows the total cross-section of carbon in the energy range from 10 MeV to 100 keV, which is in good agreement with the ENDF-B evaluated curve and as accurate as any of the published data in the energy region from 200 keV to 2 MeV. The peak at channel number 1400 is due to the resonance at 153 keV in ^{13}C .

1.3 Fission chambers for the intercomparison of fast neutron flux density measurements (D. B. Gayther)

Six laboratories* have now participated in this intercomparison and two short final measurements have been made on HELIOS to end the exercise. Financial considerations restricted the time available for the Harwell runs.

*NBS: National Bureau of Standards (USA), BIPM: Bureau International des Poids et Mesures (France), PTB: Physikalische Technische Bundesanstalt (FRG), CBNM: Central Bureau for Nuclear Measurements (EEC, Belgium), ETL: Electrotechnical Laboratory (Japan), NPL: National Physical Laboratory (UK).

It was, however, demonstrated that the chambers were operating satisfactorily at the highest intercomparison energy of 14.8 MeV which, on the 44 m flight path used, is at a flight time less than 700 ns after the "gamma-flash" passes through the chamber.

In making the intercomparison, the quantity which is studied is the neutron detection efficiency of each chamber (defined as the quotient (fission events)/(incident neutron fluence)). Figure 1.3 shows a preliminary comparison of the sensitivities obtained for the ^{235}U chamber by the six laboratories. It can be seen that there are no large discrepancies, and that the calculated sensitivity based on the ENDF/B-VI evaluated fission cross-section is close to the mean sensitivity.

When the Harwell data have been analysed it is hoped to publish the results of the intercomparison in Metrologia.

1.4 Resonant neutron capture gamma-ray spectroscopy studies in the structural materials (S. Croft and L. C. Pratt (Queen Mary College))

Last year a number of fundamental improvements to the data acquisition and data reduction systems were reported (UKNDC(87)P115, p.7). Using this improved set-up neutron capture gamma-rays have been observed from the capture resonances in ^{52}Cr and ^{54}Fe using the Fast Neutron Target of the Harwell electron linear accelerator HELIOS as a source of pulsed neutrons. These data were collected on the 12.4 m flight path F2. The gamma-rays were detected by a pair of 110 cm³ HPGe spectrometers flanking the enriched oxide samples. For each sample data were recorded over a period equivalent to approximately 10 days running time with an electron beam power of 3 kW. For the ^{52}Cr sample an electron pulse

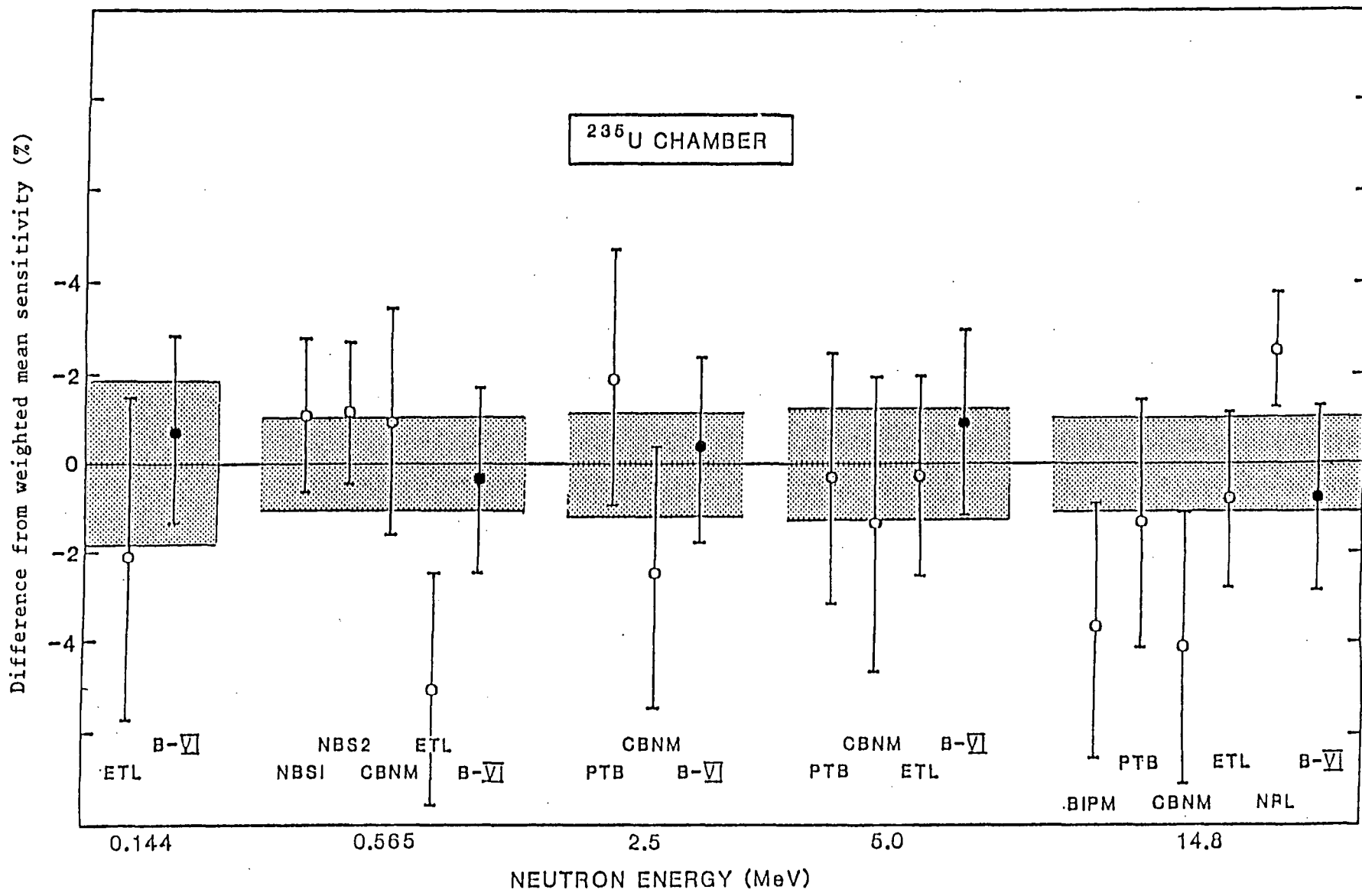


Figure 1.3. Preliminary comparison of measured fission chamber neutron sensitivities (open circles). The solid circles are the calculated sensitivities based on the ENDF/B-VI fission cross-section and the known mass of ²³⁵U in the chamber. The shaded area is the uncertainty in the weighted mean.

width of 8-10 ns was used and the time-of-flight histogram extended from 0.5 keV to 130 keV. For the ^{54}Fe sample the pulse width was between 10-12 ns and the time-of-flight histogram extended from 0.5 keV to 110 keV.

The upper energy limit is set by the recovery time of the detectors following the gamma-flash. Analysis of the ^{54}Fe data has not yet begun although it is expected to provide values for the relative strengths of high energy primary transitions from the s-wave resonances at 7.68, 52.9, 71.75 and 98.66 keV.

Analysis of the ^{52}Cr data is nearing completion. Table 1.4 shows the results obtained for capture in the 1.626 keV ^{52}Cr resonance, together with the results of Kopecky et al⁽¹⁾. There appears to be reasonably good agreement between the two data sets and this is taken as validation in our experimental arrangement and analysis codes.

Despite its technological and theoretical importance, no other spectrum measurements of resonance capture in ^{52}Cr have been reported. Consequently, when our analysis is completed we will be breaking new ground. It is intended to compare the transition strengths of the s-wave resonances with the prediction of direct capture calculations.

(1) J. Kopecky, R. E. Chrien and H. I. Liou, Nucl. Phys. A334 (1980) 35-44.

Table 1.4 Primary gamma-rays from the $^{52}\text{Cr}(n,\gamma)^{53}\text{Cr}$ reaction at 1.626 keV

E_x (keV)	E_γ (keV)	Relative Transition Intensities, I_{rel} (%)	
		Kopecky et al*	This work
0	7939.7	100.0±5.2	100.0±7.4
564	7375.6	46.5±2.9	35.8±4.2
1006	6933.3	54.1±2.9	48.4±5.9
1974	5966.1	60.5±2.9	54.9±5.4
2320	5619.3	22.7±2.3	8.1±2.9
2670	5270.6	20.3±4.1	10.0±3.3
2708	5231.0	37.8±4.7	20.0±2.6
3180	4759.8	45.3±2.9	38.4±4.4
3262	4677.7	82.6±3.5	76.1±7.3
3616	4324.8	18.0±4.7	5.0±4.6
4187	3753.5	37.2±6.4	11.7±2.4
4294	3646.4	18.0±3.5	26.6±5.7

*J. Kopecky, R. E. Chrien and H. I. Liou, Resonance neutron capture in ^{52}Cr , Nucl. Phys. A334 (1980) 35-44.

1.5 The use of neutron intensity calibrated $^9\text{Be}(\alpha,n)$ sources as 4438 keV gamma-ray reference standards (S. Croft)

(α,n) neutron sources made from an intimate mixture of a long-lived α -emitting actinide and a suitable low-Z target material are in widespread use for a variety of applications. They may be used as neutron fluence standards and to establish reference neutron fields since their neutron energy spectra are reproducible and well studied and because their strength changes in time in a predictable way. Beryllium is the most important target because it offers the highest neutron yield. ^{241}Am has been adopted by many laboratories as the alpha emitter because it has a convenient half-life (433 y), is readily available, emits a hard alpha spectrum and presents a favourably low associated gamma-ray hazard.

${}^9\text{Be}(\alpha, n)$ sources not only emit neutrons but also give off penetrating gamma-rays of 4438 keV. This fact, which has been exploited in a number of industrial instruments, suggests the possibility of using neutron intensity calibrated ${}^9\text{Be}(\alpha, n)$ sources as 4438 keV gamma-ray reference standards. The need for accurate gamma-ray intensity standards suitable for the field calibration of detectors in the energy regime above 2.5 keV is of great importance for quantitative gamma-ray spectroscopy. In many such applications it is not always possible to calibrate the system in the actual experimental arrangement to be used, using conventional accelerator or reactor based gamma-sources.

In this work an accurate measurement of the 4438 keV gamma-ray to total neutron output ratio, $R = S_\gamma/S_n$, for a commercially obtained $3\text{mCi } {}^{241}\text{Am}/{}^9\text{Be}(\alpha, n)$ source has been made. The result has been compared with those of other workers and with an extensive series of theoretical calculations. The calculations demonstrated that R is relatively insensitive to either the choice of alpha emitter or to the particulate size of the alpha emitting material. Consequently, provided details of the source fabrication and encapsulation are known and appropriate corrections are applied, the use of the product $R \times S_n$ as a means of deducing the gamma-ray yield from a neutron intensity calibrated ${}^9\text{Be}(\alpha, n)$ source would appear to be a legitimate practice. The experimental work involved determining the absolute neutron yield of the source by a technique directly traceable to the NPL MnSO_4 bath. The absolute yield of 4438 keV gamma-rays was measured using a 101 cm^3 high purity germanium detector. Particular attention was paid to the estimation of a number of source dependent correction factors including those for: the attenuation of neutrons and gamma-rays in the source encapsulation; the production of extraneous neutrons in the source; and the influence of the finite size of the source on the gamma-ray detection efficiency.

The final result of $R = 0.591 (\pm 2.6\%)$ is in good agreement with both the values reported by other workers and with the calculated value of $R = 0.566 (\pm 10\%)$. Although 6% higher than the most recent and precise previous measurement the present experimental precision is a factor of two higher than previously reported and is considered to be less prone to systematic uncertainty.

The work reported here has been incorporated into a report⁽¹⁾ from which Figures 1.4-1.6 have been taken. Figure 1.4 shows the pulse height spectrum of the 4438 keV line obtained using the 101 cm³ HPGe detector. The peaks are significantly Doppler broadened. Figure 1.5 illustrates the calculated variation of $R(E_\alpha) = S_\gamma/S_n$ for α -particles of energy E_α completely stopping in beryllium metal. As most α -emitters likely to be used in neutron source fabrication give off α -particles of between 4.5 MeV and 5.5 MeV it is evident that the R-ratio is relatively insensitive to the choice of α -emitter. Figure 1.6 illustrates the calculated energy distribution of α -particles emerging from the particles of $^{241}\text{AmO}_2$ in the neutron source studied. Because small oxide particles are needed in order to obtain a high neutron yield the amount of energy degradation is not large. By folding the predicted α -particle emission spectrum of Figure 1.6 with the $R(E_\alpha)$ curve of Figure 1.5 the theoretical R-value of the source quoted above was obtained. Details of the calculations may be found in ref. 1.

(1) S. Croft, The use of neutron intensity calibrated $^9\text{Be}(\alpha,n)$ sources as 4438 keV gamma-ray reference standards, Nucl. Instr. and Meth. in Phys. Res. A281 (1989) 103.

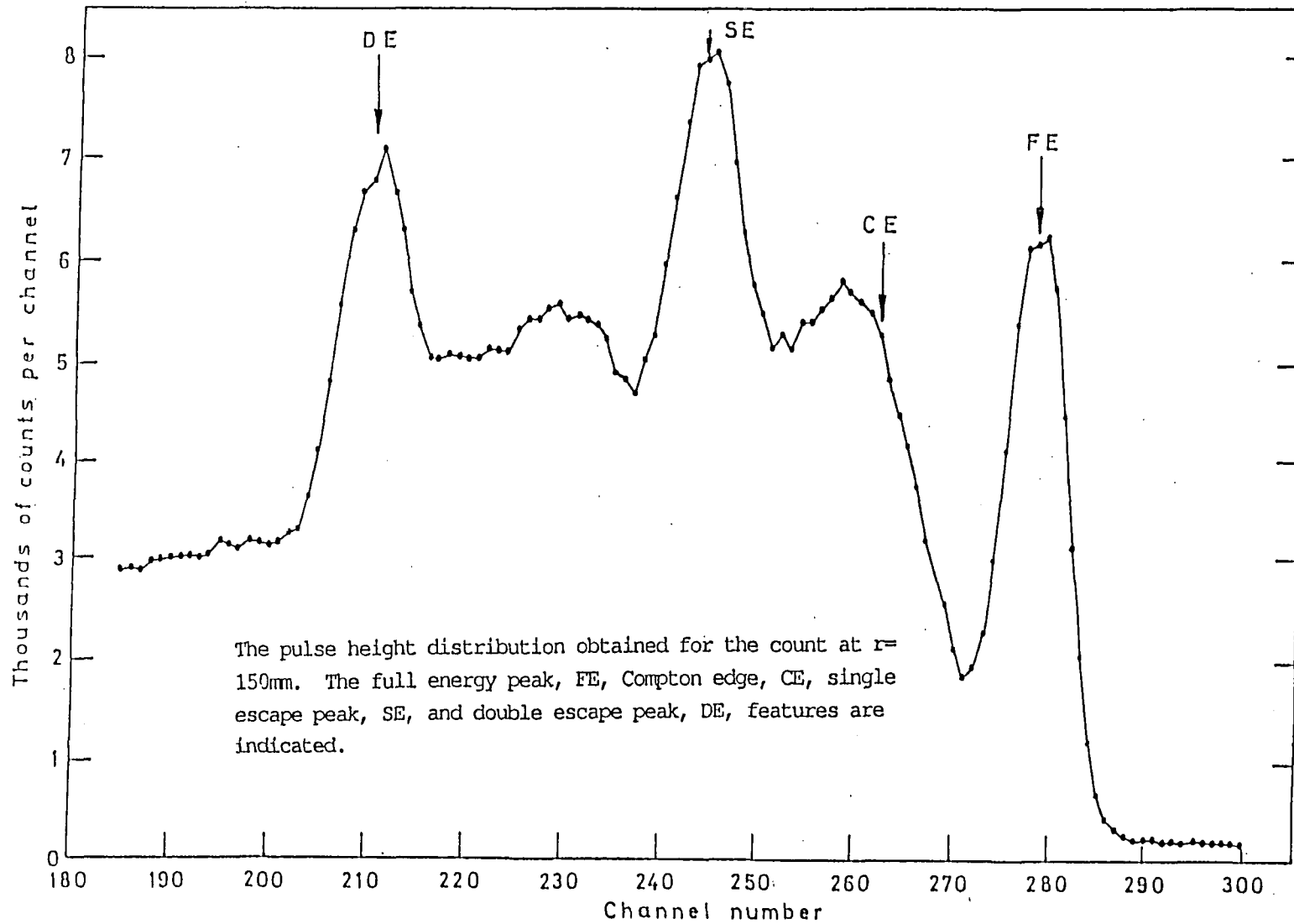


Figure 1.4

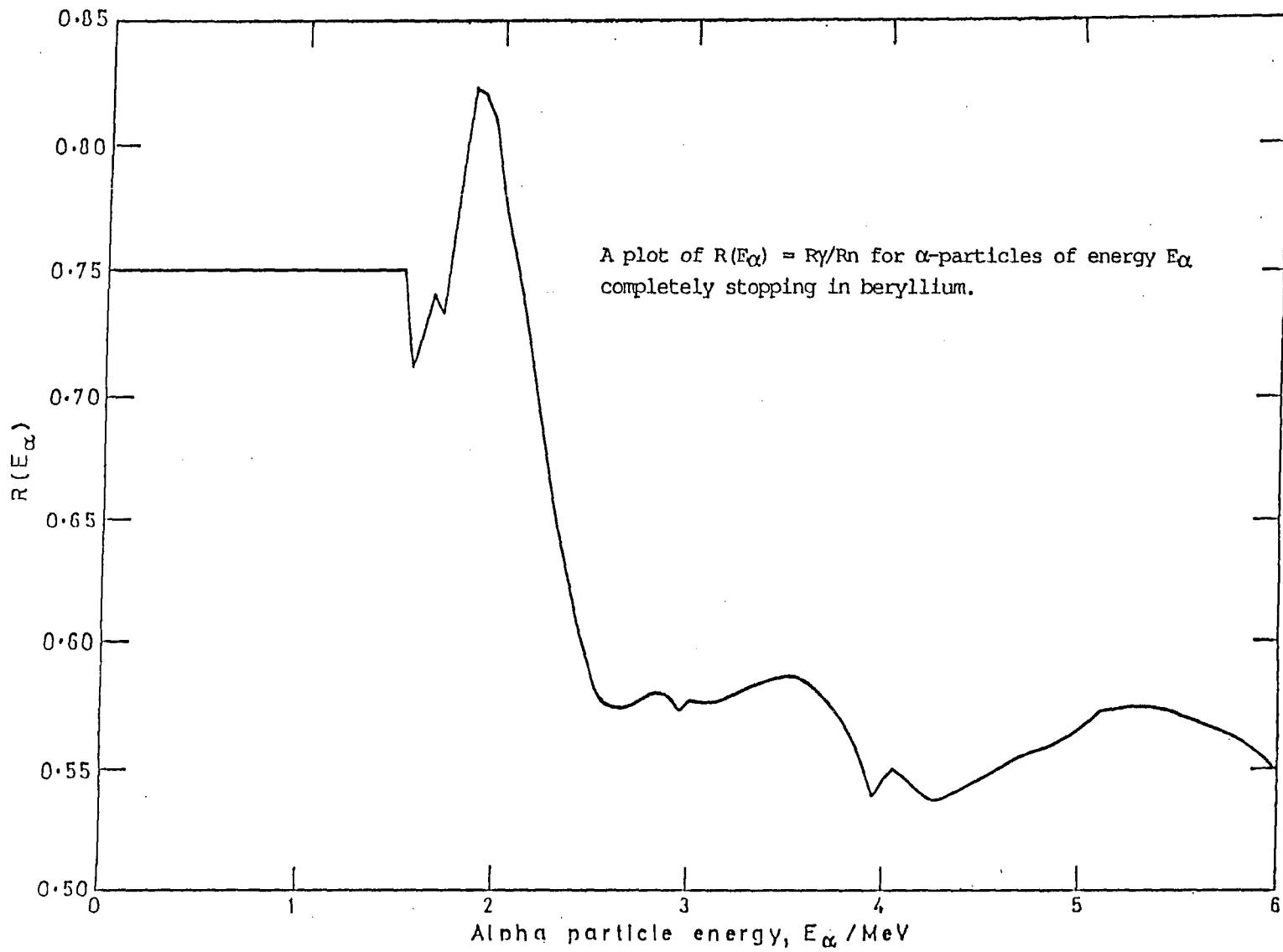


Figure 1.5

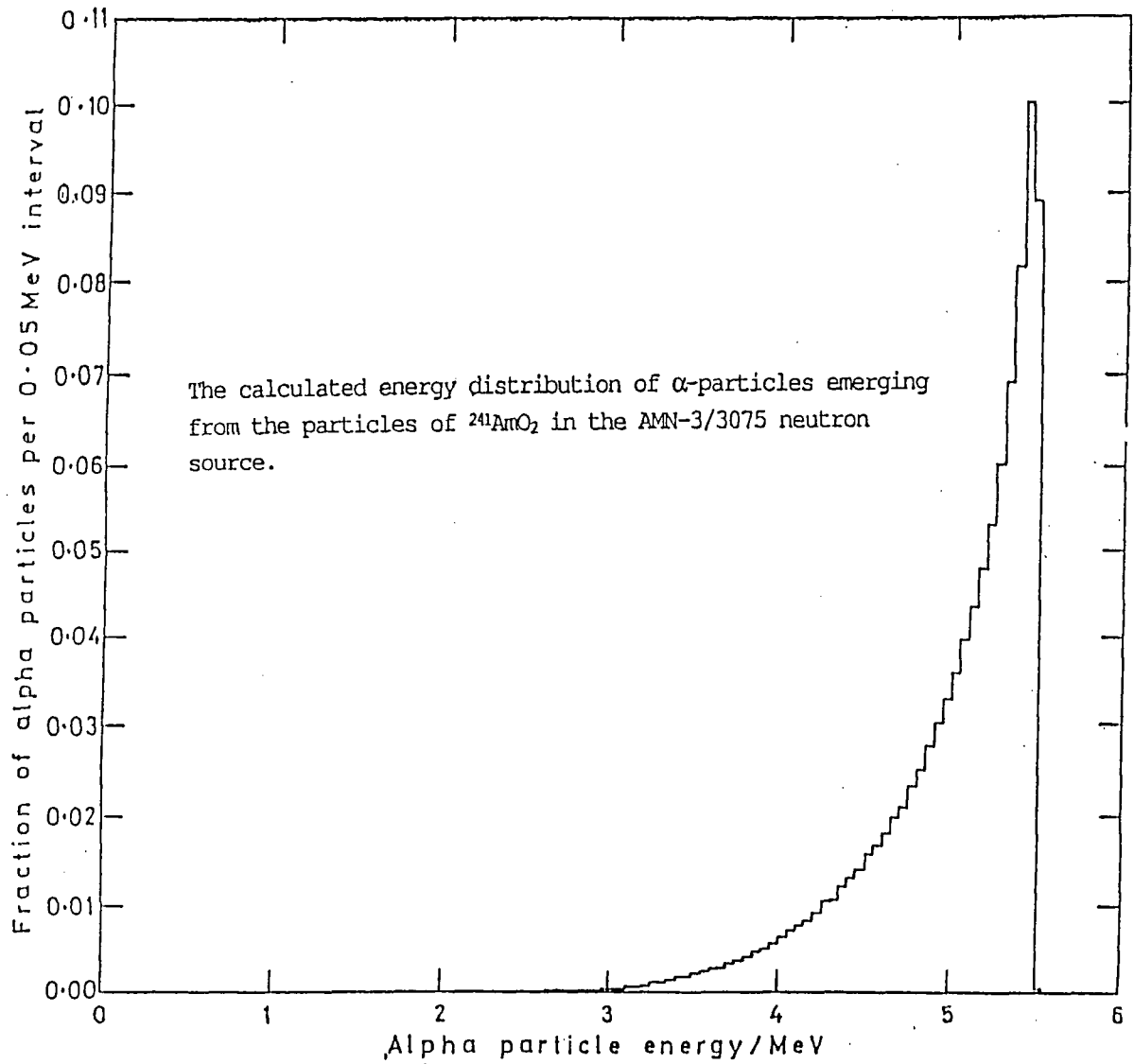


Figure 1.6

1.6 The absolute determination of the response function of the Harwell Total Energy Detector to 6.13 MeV gamma-rays (S. Croft and M. Bailey)

Accurate and precise measurements of total neutron capture cross-sections in the keV energy range are required in many areas of pure and applied science including nuclear energy level spectroscopy; neutron capture mechanism studies; stellar nucleosynthesis calculations; prompt gamma neutron activation analysis (PGNAA), and in reactor technologies such as core design and shielding. In favourable circumstances valuable information may be obtained by either neutron absorption, nuclear transmutation or neutron activation measurements. However, only the method of prompt gamma-ray detection is suitable for high resolution capture studies in the keV neutron-energy range using time-of-flight spectrometry at white neutron-source facilities. A widely used detector system for this type of work is the so-called Maier-Leibnitz Total Energy Detector, M-L TED. In this system, in addition to the neutron time-of-flight spectrum, the detectors pulse-height distribution, PHD, is also recorded. By folding the PHD with a suitably chosen weighting function, WF, the efficiency of detecting a capture gamma-ray can be made independent of the details of the cascade from which it came.

M-L TEDs based on small cylindrical cells of non-hydrogenous liquid scintillators have become widely used in many laboratories throughout the world because they combine the advantages of low cost, good time resolution and low neutron sensitivity with reasonably high detection efficiencies and low cosmic-ray background sensitivities.

The WF may be derived from the absolute PHD produced by monoenergetic photons born in the capturing sample. However, because clean, monoenergetic,

high-energy radionuclide gamma-ray sources do not exist, it is not possible to measure the response matrix of a detector in the actual experimental arrangement over the entire energy range of interest. Consequently the monoenergetic response functions used to date have been generated almost exclusively by Monte-Carlo simulation.

It is believed that the long-standing discrepancy between the resonance parameters of the 1.15 keV resonance in ^{56}Fe derived from transmission and recent capture measurements is the result of not taking proper account of the capture gamma-ray interactions in, and the subsequent electron migration from, the materials close to the capture samples and the capture detectors (UKNDC(87) P115, p.3). This is because these processes affect both the shape and absolute normalisation of the PHDs. In order to confirm these conjectures the absolute response function of the Harwell C_6D_6 (Figure 1.7) M-L TED to essentially monoenergetic 6.13 MeV gamma-rays has been measured and comparisons have been made with spectra generated using the comprehensive Monte-Carlo electron-gamma tracking code EGS-4⁽¹⁾.

The experiment was performed using a nearly monoenergetic and isotropic photon field produced using the $^{19}\text{F}(p,\alpha\gamma)^{16}\text{O}$ reaction by bombarding a thin CaF_2/Ta target with 375 keV protons from the Harwell 5 MV Van de Graaff accelerator. The absolute yield of photons was measured using a 101 cm³ HPGe gamma-ray spectrometer whose efficiency had been previously determined using a combination of radionuclide and thermal neutron capture gamma-ray sources. A secondary calibration, based on measurements with a standard 3" x 3" NaI(Tl) scintillator gave consistent results.

(1) S. Croft and M. Bailey, The determination of the absolute response function of a deuterated benzene total energy detector to 6.13 MeV gamma-rays. In preparation.

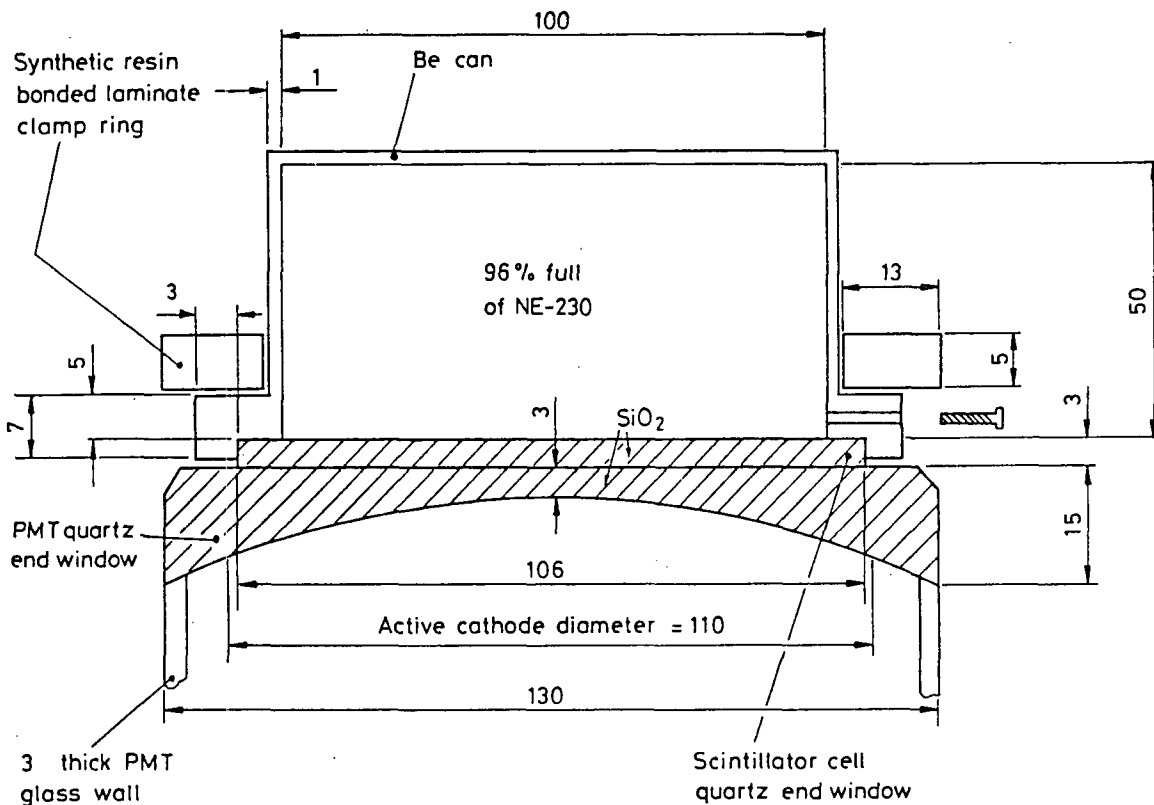


Figure 1.7

A particularly open irradiation geometry (Figure 1.8) was used so as to minimise the importance of scattered radiation and to enable the geometry to be accurately represented in the computer simulations. Even so the 0.265 mm Ta target backing was shown to be a significant electron radiator. An aluminium absorber placed in front of the detector was found to drastically reduce the continuum in the PHD caused by these electrons.

Table 1.5 gives a comparison of the absolute detection efficiencies predicted using the EGS-4 code and those actually observed. In both cases the detector was mounted at an angle of 45° with respect to the proton beam and at a distance of 112 mm from the target. The overall uncertainty associated with the experimental results is $\pm 5.4\%$. This is dominated by the uncertainty in the

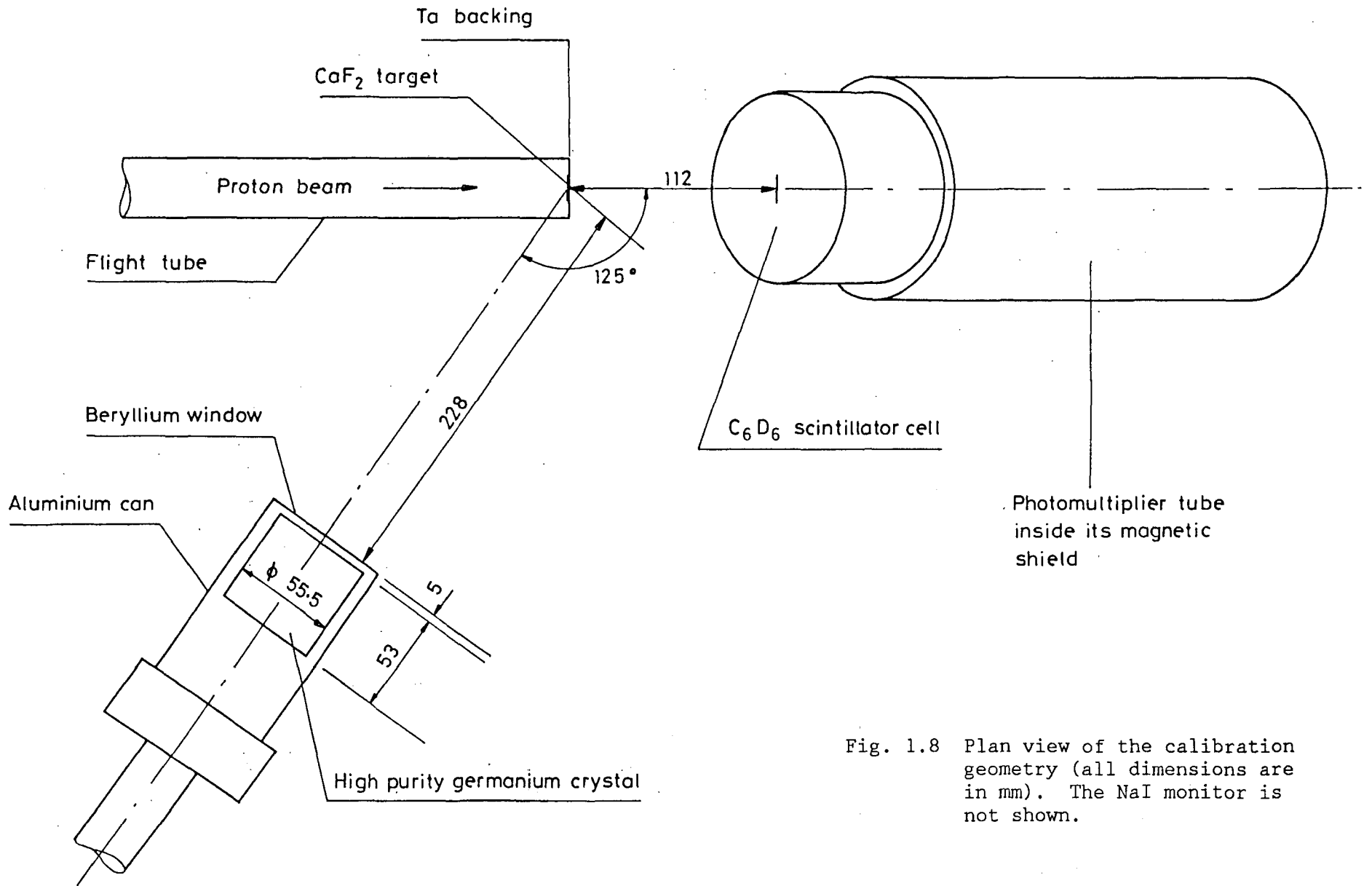


Fig. 1.8 Plan view of the calibration geometry (all dimensions are in mm). The NaI monitor is not shown.

Table 1.5

A comparison of the total detection efficiency as a function of detection threshold using the EGS-4 code and measured in the present experiment. The C_6D_6 TED was located 112 mm from the target with its axis at 45° to the proton beam direction. The calculations refer to an isotropic source of 6.13 MeV photons 6 mm in diameter. The accuracy of these values is discussed in the text.

Bias (keV)	Detection Efficiency, ϵ (%)		Ratio Measured to Calculated Efficiencies
	EGS-4	Measured	
0	0.659	0.7458	1.132
50	0.628	0.7277	1.159
100	0.606	0.7141	1.178
150	0.589	0.7014	1.191
200	0.577	0.6859	1.189
250	0.568	0.6745	1.188

absolute calibration of the HPGe detector (5.1%). The uncertainty in the EGS-4 results is difficult to assess but is believed to be less than 5%. Agreement is therefore at about the 2.6σ level. This is considerably better than the agreement obtained in the past using a variety of ad hoc codes which could not reproduce to absolute efficiency to within a factor of 2.5.

The influence of the Ta target backing is clearly shown in Table 1.6 which contains the results of a series of EGS-4 calculations. Experiments undertaken using target backings of 0.265 mm and 1.06 mm thick Ta demonstrated that the difference between these two cases is indeed not great. However, the presence of tantalum and other structural materials in the vicinity of the detector is evidently very important and represents a severe test, since the electron tracking routine of any simulation code is used to model the detector response. The implication here is that great care must be taken in generating response functions for capture detectors in realistic capture geometries.

Table 1.6

The effect of the Ta target backing and pulse-height bias on the total detection efficiency as calculated using the EGS-4 code. The C_6D_6 TED was located 112 mm from the target with its axis at 45° to the proton beam direction. The calculations refer to an isotropic source of 6.13 MeV photons 6 mm in diameter. The efficiency values listed are the absolute number of pulse-height events recorded above the bias per source photon released and are expressed in %. The figures in brackets are the % statistical standard deviations associated with the efficiency values; these are approximately the same for all biases.

Ta thickness (mm)	Bias (keV)					
	0	50	100	150	200	250
0.000	0.3532 (2.4)	0.3424	0.3358	0.3296	0.3232	0.3184
0.060	0.4808 (2.0)	0.4680	0.4560	0.4454	0.4360	0.4304
0.121	0.5442 (1.9)	0.5286	0.5192	0.5082	0.5004	0.4932
0.265	0.6589 (0.90)	0.6279	0.6064	0.5899	0.5774	0.5676
0.600	0.7278 (1.7)	0.6792	0.6472	0.6224	0.6040	0.5842
1.000	0.7646 (1.6)	0.7016	0.6582	0.6250	0.5992	0.5786

The sensitivity of the detection efficiency of the experimental arrangement is emphasised in a different way in Figure 1.9 which shows the effect of rotating the target from 45° to 90° with respect to the proton beam. At the 90° position the effective thickness of tantalum is considerably larger, with the result that electron migration becomes more significant and gives rise to more low pulse-height events.

Figure 1.10 illustrates how, by introducing 12 mm of aluminium in front of the C_6D_6 scintillator, the contribution of scattered to the PHD can be dramatically reduced. In this figure the detector was mounted at 45° to the proton beam at a distance of 150 mm from the source.

Finally Figure 1.11 shows the overall agreement between the measured PHD and that calculated using EGS-4 taking into account all the important materials in the neighbourhood of the detector. Although there are detailed differences in the shape, the overall agreement is considered to be satisfactory. It may be possible to improve the fit by including in the calculation details of the scintillation light collection processes. However, as the shape of the weighting function is particularly reliant on the variation of the efficiency with gamma-ray energy, this may not be essential before a reliable WF may be derived using monoenergetic response functions generated using the EGS-4 code.

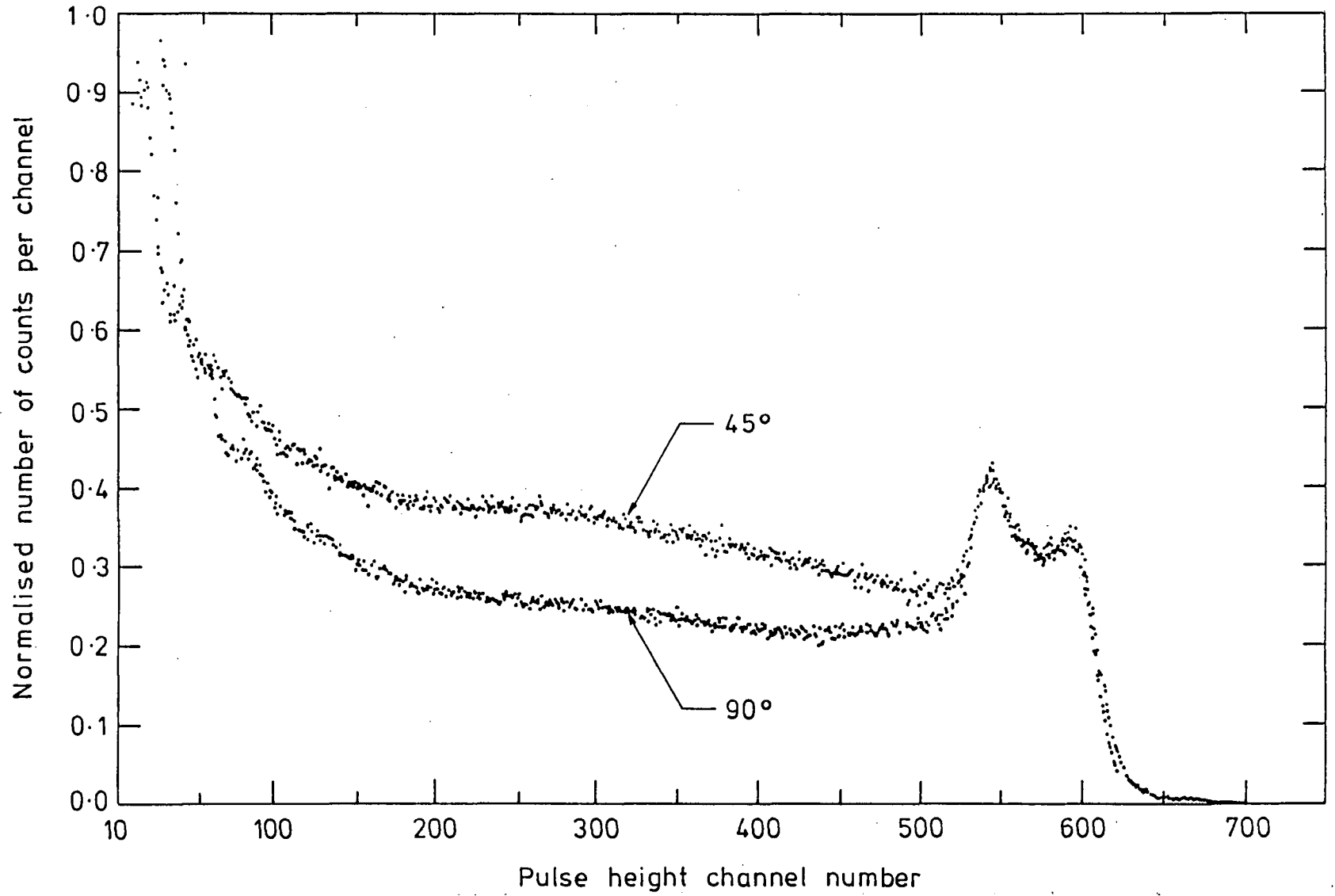


Figure 1.9 The effect of detector orientation

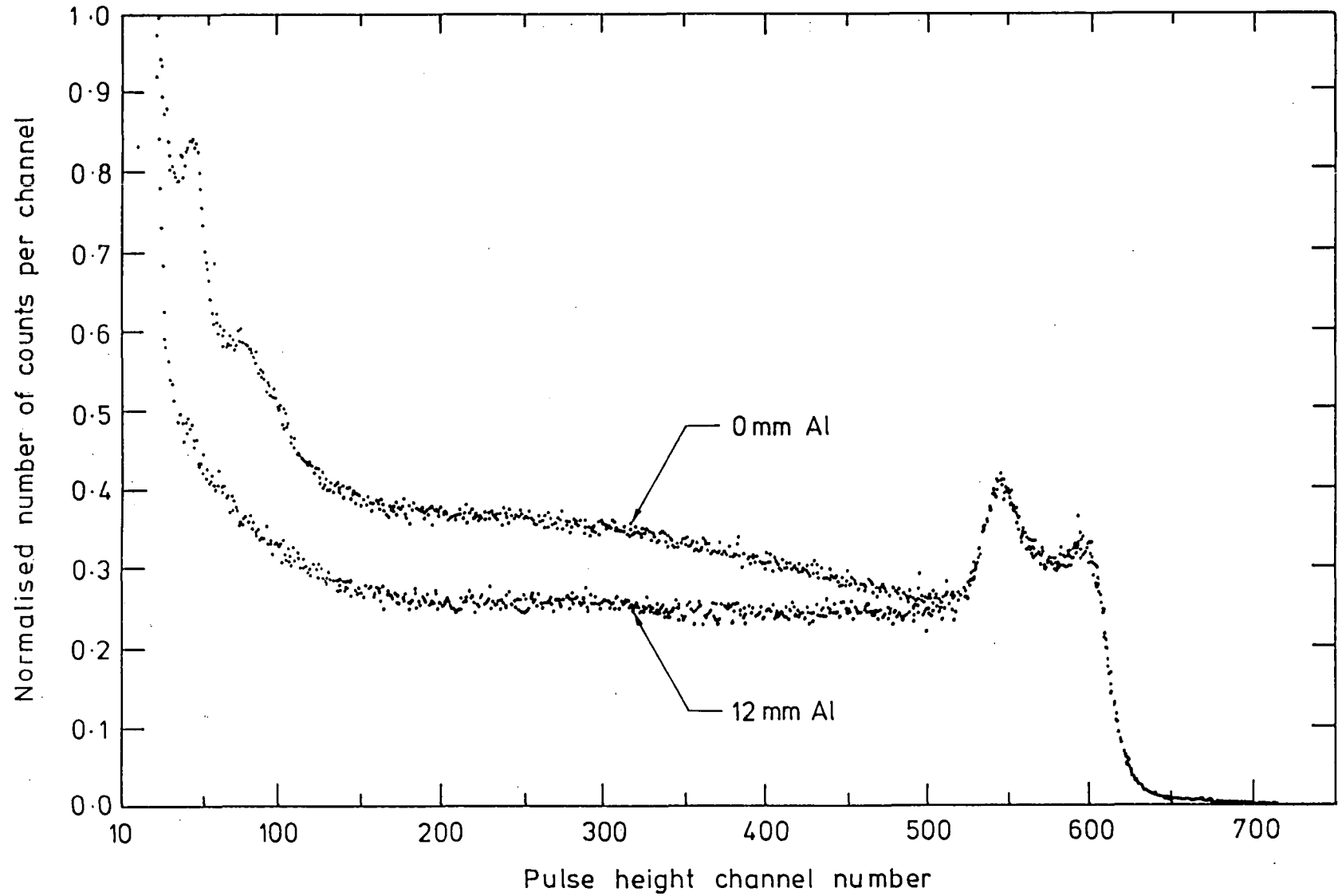


Figure 1.10 The effect of introducing 12 mm of Al in front of the detector

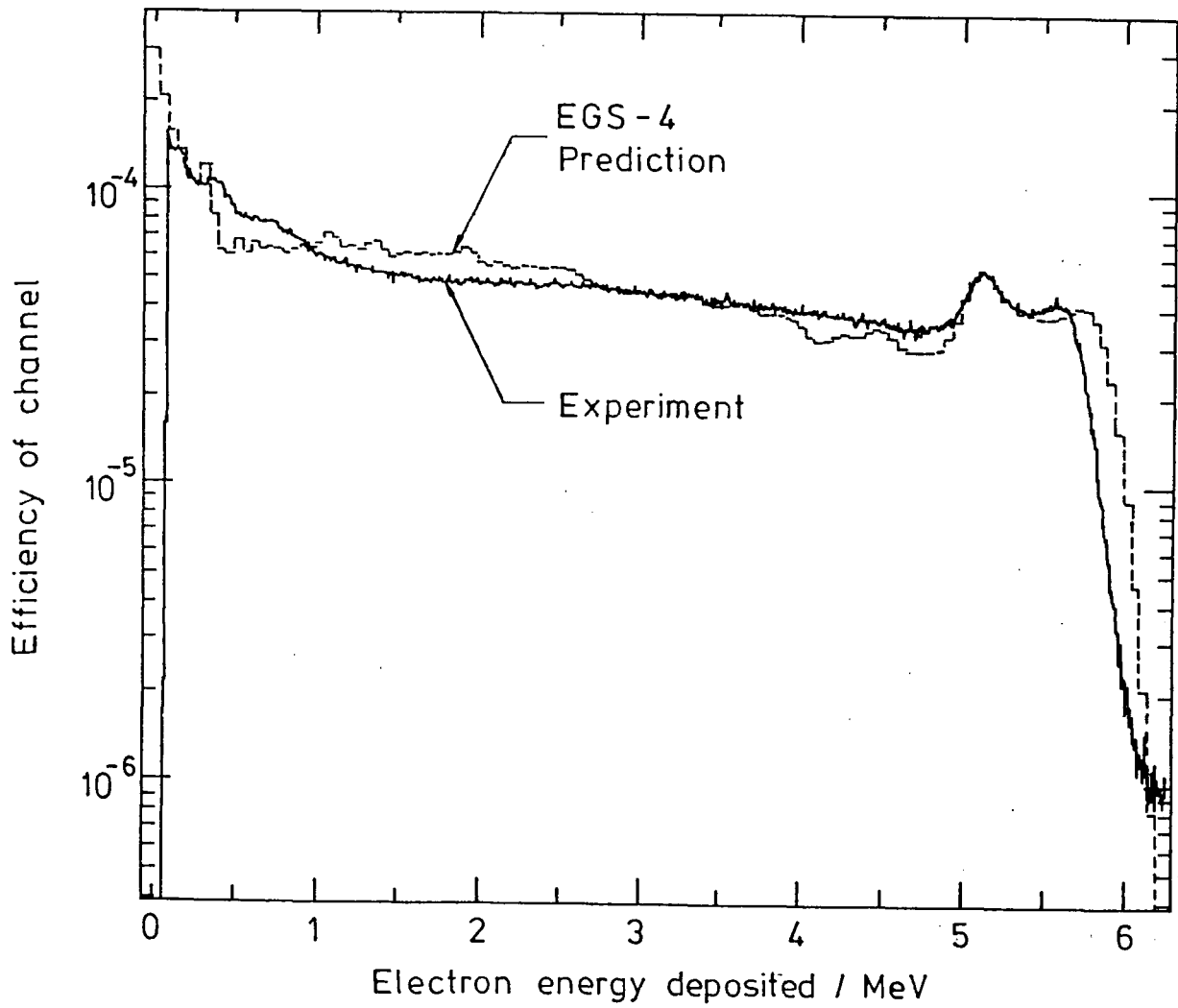


Figure 1.11 A comparison of the measured and calculated PHDs for the Harwell C_6D_6 TED mounted at 45° with respect to the proton beam 112 mm from the 6 mm diameter source. The target backing was 0.265 mm of Ta.

1.7 The potential for making accurate absolute measurements of the HELIOS neutron spectrum below 200 keV using a ^{10}B sample and a pair of high purity germanium gamma-ray spectrometers (S. Croft and M. C. Moxon)

The reduction of capture, neutron and other reaction product yield data to absolute neutron cross-section values requires an absolute determination of the neutron fluence to be made. Below 200 keV the $^{10}\text{B}(n,\alpha)^7\text{Li}$ cross-section is a recognised standard⁽¹⁾.

It has been shown that, by detecting the 477.6 keV gamma-rays emitted from a 0.99 mm thick sample of enriched ^{10}B in a calibrated detector, it is possible to measure the absolute HELIOS neutron spectrum below 200 keV with an uncertainty of less than about 2.5%.

The preliminary work reported here has been directed towards assessing the importance of a number of small correction factors and in determining the ^{10}B content of the B-sample.

The B-sample consists of 7.35 g of finely powdered B-metal uniformly compacted and sealed into a cylindrical aluminium can 86.5 mm in diameter. The can walls are 0.260 mm thick. The boron was enriched to 95.2 atom. % ^{10}B and a chemical analysis showed that 95.59 weight % of the material was B, the remainder being Mg 1.30 weight.%, Fe 0.27 weight.% and O 0.84 weight.%.

In order to obtain an accurate value of the ^{10}B content of the sample and to check its uniformity, the neutron transmission of the sample was measured as

(1) E. Wattecamps, 'The $^{10}\text{B}(n,\alpha)$ cross-section', IAEA Tech. Report 227 (1983) 19-23.

a function of energy over the energy range 0.1 eV to 100 eV. Data were collected simultaneously at the 8.8 m and 14.7 m ⁶Li-glass detector stations of the transmission spectrometer on the Condensed Matter Target of HELIOS. The energy calibration of the flight path was achieved by analysing the position of narrow resonance dip minima in isotopes of Hf, Gd, Ag and Co. The background was determined using the black filter technique using resonances in Ag, Cd, Hf and Co. The transmission data were analysed according to the following set of equations:

$$T = e^{-n\sigma}$$

$$\begin{aligned} \ln(1/T) &= (n\sigma) = a + (b/\sqrt{E}) = a + b(t-t_0)/(CL) \\ &= (a-(t_0/CL)) + b/(CL).t \\ &= n_{Al} \cdot \sigma_{Al}(E(\text{eV})) + \\ &= n_{10}(\sigma_{10,s} + \alpha + (\sigma_{10,\alpha} + \beta/\sqrt{E}(\text{eV}))) \end{aligned}$$

where (CL) is a constant related to the flight path length and determined in the energy calibration experiment; t_0 is the timing off-set determined in the energy calibration experiment; a and b are constants to be determined; n_{Al} is the number of atoms per barn value of the Al can; $\sigma_{Al}(E(\text{eV}))$ is the total neutron cross-section in barns of aluminium at the neutron energy $E(\text{eV})$; n_{10} is the number of atoms per barn of ¹⁰B in the sample; $\sigma_{10,s}$ is the scattering cross-section of ¹⁰B; $\sigma_{10,\alpha}$ is the (n, α) cross-section of ¹⁰B at 1 eV. α and β are small corrections which take account of the presence of impurities in the sample.

The result of the fit is shown in Figure 1.12. The n-value obtained was 6.9592×10^{-3} with an uncertainty of only $\pm 0.64\%$ ($\pm 0.25\%$ associated with the fit, $\pm 0.31\%$ associated with the ¹⁰B cross-section and $\pm 0.50\%$ associated with the sample uniformity).

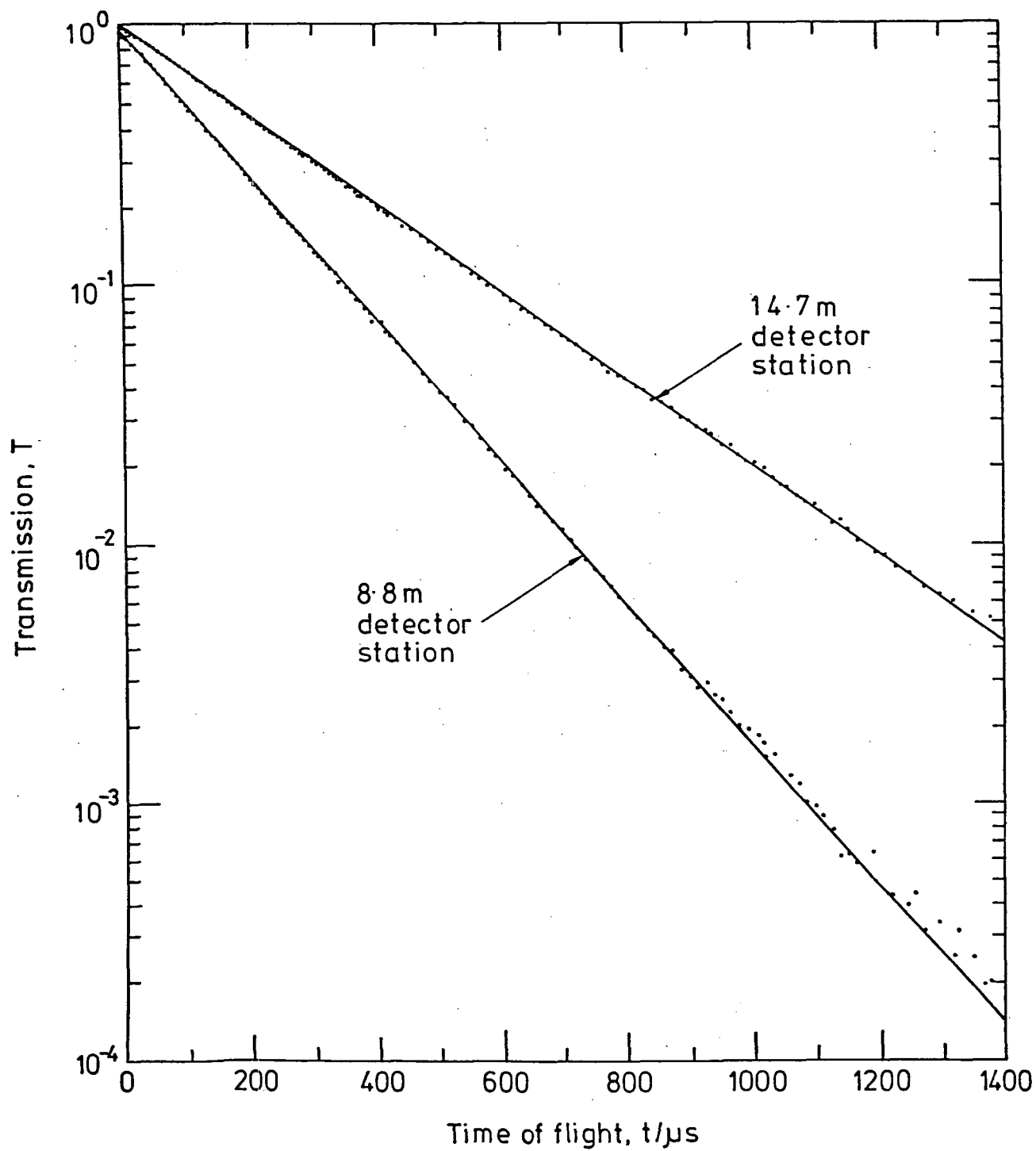


Figure 1.12 Fit to neutron transmission of ^{10}B sample of form described in the text.

Table 1.7 shows how the uncertainty in the n_{10} -value combines with other factors to give an overall uncertainty of less than 2.5% in the measurement of absolute neutron spectra on HELIOS.

The multiple scattering correction is less than 3% over the energy range of interest and can be accurately calculated using the sub-routine MULS associated with the resonance analysis code REFIT⁽¹⁾.

A Monte Carlo programme has been written to calculate the transmission of the sample for 477.6 keV gamma-rays taking into account the spatial dependence of the birth distribution brought about by the non-uniformity of the incident neutron beam and by the absorption of neutrons within the sample. Initial results indicate that a correction of only about 1.2% is necessary.

The important thing to realise is that by using extended ⁷Be sources the gamma-ray detection efficiency of the HPGe detectors can be measured directly at 477.6 keV in a realistic geometry. Consequently systematic errors associated with determining the efficiency using point sources of some other energy are avoided.

(1) M. C. Moxon, 'REFIT - a least squares fitting program for resonance analysis of neutron transmission data', Proc. Conf. on Neutron Data of Structural Materials for Fast Reactors, Geel, December 1977, published as "Neutron Data of Structural Materials for Fast Reactors", K. H. Böckhoff (ed.), Pergamon Press, Oxford (1978).

Table 1.7

A breakdown of the uncertainties contributing to the absolute neutron fluence determination

	1 keV ↓		200 keV ↓
$^{10}\text{B}(n,\alpha_1)$ cross-section, $\sigma_{n\alpha_1}$	±0.3	-	1.2%
Energy calibration of the TOF line, E_n	±0.17		
n_{10}	±0.64		
Multiple scattering correction, α_{tot}	±0.20	-	0.30%
Gamma transmission, T_γ	±0.12		
Background neutron subtraction	±0.2		
FEP efficiency determination, ^7Be	±1.5		
Counting statistics, 5000 counts.channel ⁻¹	±1.4142	=	$\sqrt{2}$
FC monitor stability used for run normalisation	±0.2		
	2.22	-	2.51%

1.8 Evaluation of cross-sections for the Joint Evaluated File (M. C. Moxon, M. G. Sowerby, J. B. Brisland and D. A. J. Endacott)

Standard Cross-sections

In view of our involvement with the Phase 1 review of the ENDF/B-VI standard cross-sections we now have the informal responsibility of keeping the JEF project informed and making any necessary recommendations on these standards. In the Phase 1 review (see UKNDC(87)P115, p.2) we found that the ^{238}U capture cross-section, which was evaluated with the standards, was incorrect. Further

interaction with the US evaluator has resulted in the cross-section being revised and the final recommendations are now acceptable. However, the cross-section still tends to be lower than many of the measurements, which is not completely unexpected when the data are evaluated simultaneously with other cross-sections, but it does make further accurate ^{238}U capture cross-section measurements highly desirable.

^{238}U Cross-sections

Most of our work has continued to be in the resolved resonance range, where it is being done in cooperation with the NEA Data Bank. A preliminary set of resonance parameters was produced at the end of 1987 based on the data in Table 1.8. Unfortunately only a preliminary set of data was available from Macklin et al and when the final data became available at about the same time it was clear that the new data differed significantly from the old values particularly above 9 keV. The data of Macklin et al play a key role in the analysis at high energies because many resonances are not seen in the transmission data. Olsen⁽¹⁾ for example only produced the parameters of 676 resonances in an analysis of the transmission data of Olsen et al⁽²⁾ between 0.9 and 10 keV (-1800 s- and p-wave resonances are expected in this energy range for an s-wave level spacing of 20 eV). It can be seen in Figure 1.13, which compares the transmission and capture yield data of Olsen et al⁽²⁾ and Macklin et al⁽³⁾ respectively, that many of the missed resonances are seen in the capture data. In the energy range 9180 to 9320 the transmission can be fitted

(1) D. K. Olsen, Nucl. Sci. Eng. 94 (1986) 102.

(2) D. K. Olsen, G. de Saussure, R. B. Perez, F. C. Difilippo, R. W. Ingle and H. Weaver, Nucl. Sci. Eng. 69 (1979) 202.

(3) Roger L. Macklin, R. B. Perez, G. de Saussure and R. W. Ingle, Paper AA07 presented to International Conference on Nuclear Data for Science and Technology, Mito, Japan, May 30-June 3 (1988).

by 6 resonances while the analysis shown requires 21 resonances. Between 9 and 10 keV ~36% of the capture cross-section is accounted for by resonances not seen in transmission. In view of the importance of the capture data in the analysis it was therefore necessary to reconsider the adequacy of the preliminary parameter set.

Table 1.8

Data being used in the ^{238}U resolved resonance analysis

Energy range	Capture data	Transmission data
0-900 eV	*de Saussure et al(1) **Moxon(3)	Olsen et al(4)
900-4000 eV	*de Saussure et al(1) Macklin et al(2)	Olsen et al(5)
4000-10,000 eV	Macklin et al(2)	Olsen et al(5)

*Data renormalised; **First few resonances only

The average capture cross-sections calculated from the preliminary set of parameters agree with the revised ^{238}U capture cross-section associated with

-
- (1) G. de Saussure, E. G. Silver, R. B. Perez, R. Ingle and H. Weaver, Nucl. Sci. Eng. 5 (1973) 385.
 - (2) Roger L. Macklin, R. B. Perez, G. de Saussure and R. W. Ingle, Paper AA07 presented to International Conference on Nuclear Data for Science and Technology, Mito, Japan, May 30-June 3 (1988).
 - (3) M. C. Moxon, AERE-R 6074 (1969).
 - (4) D. K. Olsen, G. de Saussure, R. B. Perez, E. G. Silver, F. C. Difilippo, R. W. Ingle and H. Weaver, Nucl. Sci. Eng. 62 (1979) 479.
 - (5) D. K. Olsen, G. de Saussure, R. B. Perez, F. C. Difilippo, R. W. Ingle and H. Weaver, Nucl. Sci. Eng. 69 (1979) 202.

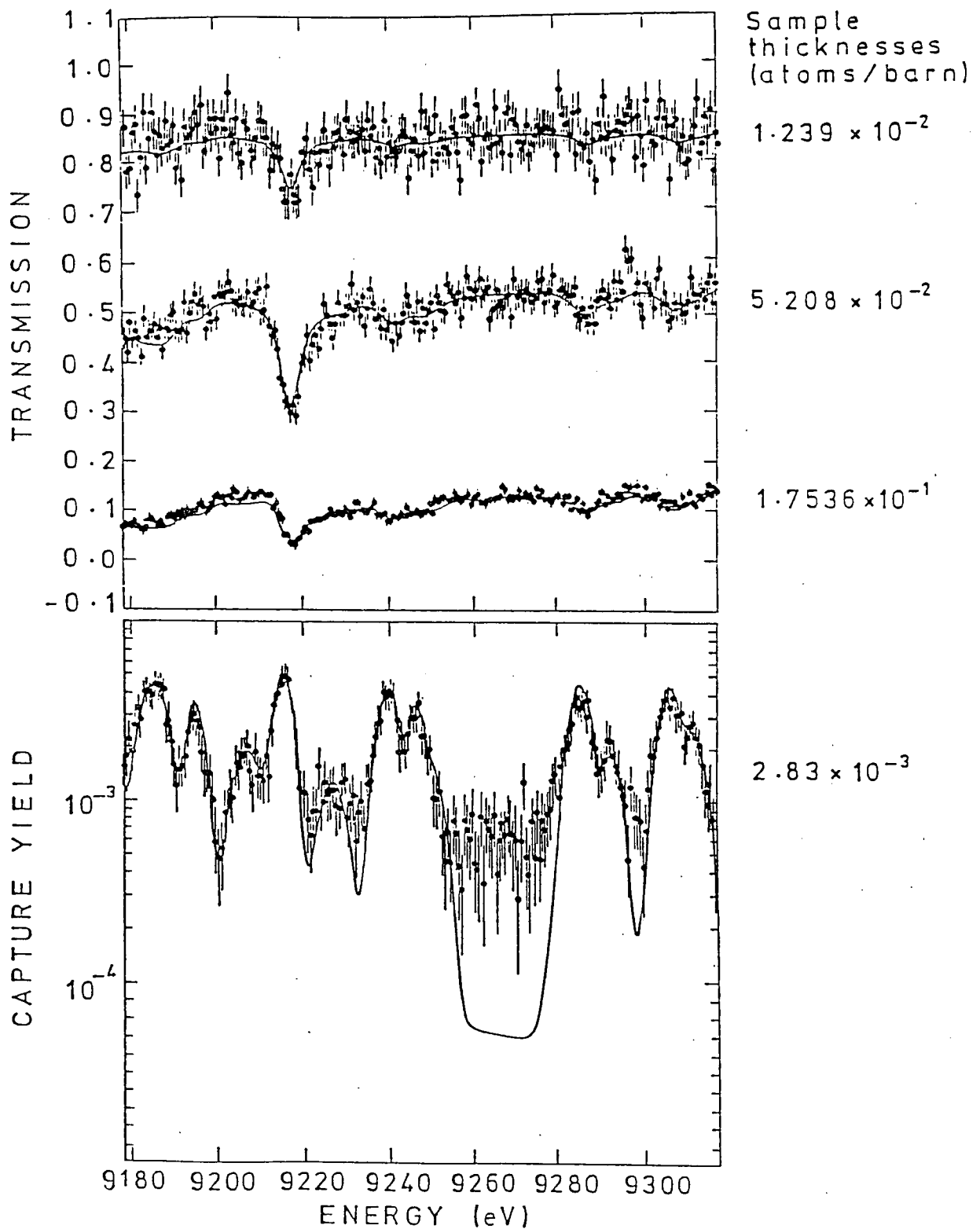


Figure 1.13 Comparison of transmission measurements of Olsen et al (Nucl. Sci. Eng. 69 (1979) 202) and the preliminary capture data of Macklin et al (Paper AA07, Mito Conf., Japan (1988)) with the values calculated from resonance parameters.

the ENDF/B-VI standards evaluation (see page 32) below 4 keV but are significantly higher from 4 to 10 keV. Investigations of these discrepancies has led us to the view that the final data of Macklin et al require both background correction and renormalisation. As a result of discussions at Oak Ridge we believe it is prudent to investigate the energy dependence of both these parameters, and this is in progress. The background correction is in principle relatively straight-forward as the level can be deduced from the capture yield between resonances. As you approach 10 keV, however, suitable energy regions for this are more difficult to find due to the worsening energy resolution combined with the increased strength of the p-wave resonances. The problem of normalisation is more difficult - even impossible approaching 10 keV - as the resonances used need to have the following properties

- (1) be isolated, with no other overlapping resonances
- (2) have $g\Gamma_n$ determined accurately from transmission measurements
- (3) have $g\Gamma_n \ll \Gamma_\gamma$ so that the capture area is independent of Γ_γ .

Suitable resonances are possible at low energies but are virtually impossible to find at high energies. Initially we attempted to solve the problem by doing resonance analysis over a number of energy ranges each of which included several resonances with a variety of Γ_n values and a wide energy region with no resonances. This method was unsuccessful because the corrections to background and normalisation turned out to be highly correlated and not therefore unique. (If all energy ranges could have been considered simultaneously the method might have been more successful.) The corrections are therefore now being investigated consecutively.

Because of the timescales of the JEF Project it will not be possible to complete all the work before the resonance parameters are needed. In view of this a set of parameters will be obtained based on some arbitrary decisions

regarding normalisation and background. In due course a more correct set will be produced which will be more physically meaningful.

A start has now been made on assembling the full ^{238}U file for JEF-2. The cross-sections in this come from a variety of sources and there are inconsistencies which are being identified and remedied. In some cases this requires further evaluation work.

1.9 FISPIN on the Harwell Computer (D. A. J. Endacott)

The FISPIN code⁽¹⁾ calculates the inventory of nuclides (fission products and actinides) following an irradiation in a fission reactor. Several versions of the code along with their data sets are maintained on the Harwell IBM 3084Q mainframe computer and these are widely used by the UK nuclear industry. In the past year, in addition to maintaining the code and its associated data libraries, assistance has been given to code users and some of the work to comprehensively document version 6 of the code has been performed. A report⁽²⁾ on this is at present in the draft stage.

1.10 Fusion reactor activation calculations (R. A. Forrest, M. G. Sowerby, B. H. Patrick and D. A. J. Endacott)

The programme of work on activation of materials in fusion reactors has continued, covering nuclear data evaluation, inventory code development and calculations.

(1) R. F. Burstall, ND-R-328 (1979).

(2) S. W. Power, R. F. Burstall, D. A. J. Endacott and P. C. Miller, RP and SG/SWP/P(89)3.

The cross-section library UKACT1 was described in last year's report (UKNDC(87)P115, p.20), where it was noted that the treatment of capture cross-sections is rather weak. Work is in hand to improve these by means of scaling parts of the data to agree with thermal and resonance integral values from existing compilations. Other improvements such as additional targets, new isomer ratio and reaction systematics and the incorporation of more evaluated files should enable UKACT2 to be completed over the next year.

To complement improvements in the cross-section data, the decay data library must also be updated. Many of the nuclides which previously had data files created by hand are being replaced by evaluated files, and detailed checking will be necessary to ensure that the identification of all nuclides (especially isomers) in both libraries is consistent. This will lead to the production of UKDECAY3.

Considerable progress has been made with the inventory code FISPACT. Version 1.3 has been fully documented by means of a Program Manual⁽¹⁾ and a User Manual⁽²⁾. This code is in regular use at Harwell, Culham and Imperial College and has proved very robust. Several new features have been included in Version 1.4, notably the introduction of Pathway Analysis, user control of convergence limits and enhanced printed and graphical output. The code has also been converted to run on an expanded personal computer and a start made on conversion to the CRAY.

-
- (1) R. A. Forrest and D. A. J. Endacott, 'FISPACT - Program Manual', AERE-M-3655 (1988).
 - (2) R. A. Forrest and D. A. J. Endacott, 'FISPACT - User Manual', AERE-M-3654 (1988).

Version 1.3 contains a sensitivity routine which calculates the effect of a change of cross-section on the amount of a particular nuclide formed during irradiation. This can however be expensive in computer time and the generated sensitivity coefficients need careful interpretation. The Pathway Analysis option introduced in Version 1.4 allows the percentage of a nuclide formed by a specified pathway (linear series of reactions and decays) to be calculated very quickly. Both these methods enable the important reactions for formation of troublesome nuclides to be identified and these can be focused on during improvement of the data library.

A further feature that it is planned to include in FISPACT is a detailed treatment of gas production. In the current versions all reactions from a parent to a daughter are summed together, e.g. (n,d) and (n,n'p) are considered as a single reaction. In reality these two reactions produce different isotopes of H as gaseous products and in the case of (n,t) reactions, the tritium formed is itself radioactive and so should contribute to the total activity of the material. The full treatment of gas production should be included in Version 1.5 of the code.

It has been noted that FISPACT and the data libraries are in routine use for calculating activation in various fusion devices. Three examples of its recent use at Harwell are the calculations presented at the Mito Conference⁽¹⁾, the activation of diagnostic equipment in the JET torus hall⁽²⁾ and a report covering activation of thirty elements in a DEMO type reactor⁽³⁾. The latter includes details of dominant pathways to long-lived

-
- (1) R. A. Forrest, M. G. Sowerby, B. H. Patrick and D. A. J. Endacott, 'The Data Library UKACT1 and the Inventory Code FISPACT', Nuclear Data for Science and Technology (Mito), 1061 (1988).
 - (2) R. A. Forrest, B. H. Patrick, M. G. Sowerby and D. A. J. Endacott, 'Activation of Material in the JET Torus Hall', JDECOM(88)23 (1988).
 - (3) R. A. Forrest and D. A. J. Endacott, 'Activation Data for Some Elements Relevant to Fusion Reactors', AERE Report in preparation (1989).

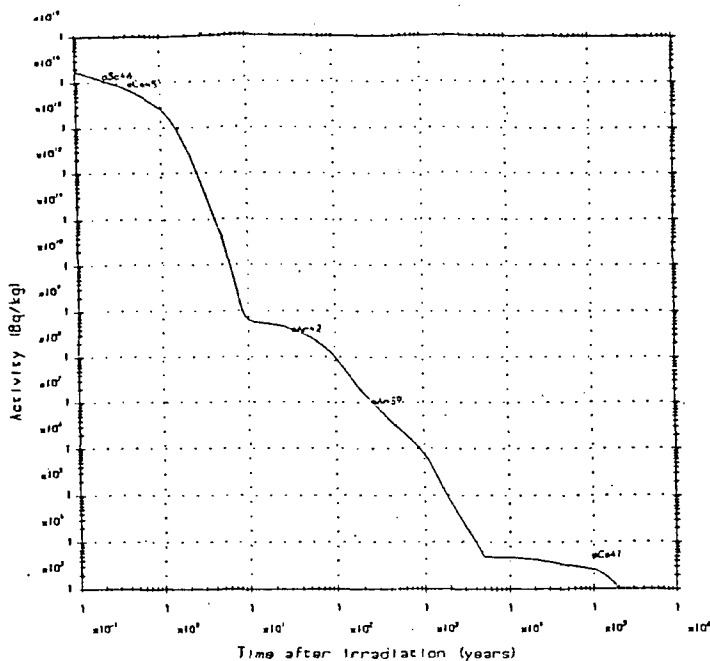
nuclides, in addition to tabulations of activities, dose rates, biological hazard indices and afterheat. The data for irradiation of titanium are shown in Figure 1.14.

In order to ensure that FISPACT has a wide usage by the international fusion community the code and data have been supplied to two European laboratories (KfK and ECN Petten) which are collaborating with Harwell. The code will also be generally available from the NEA Data Bank in the near future.

Figure 1.14 Data from FISPACT for irradiation of titanium

TITANIUM

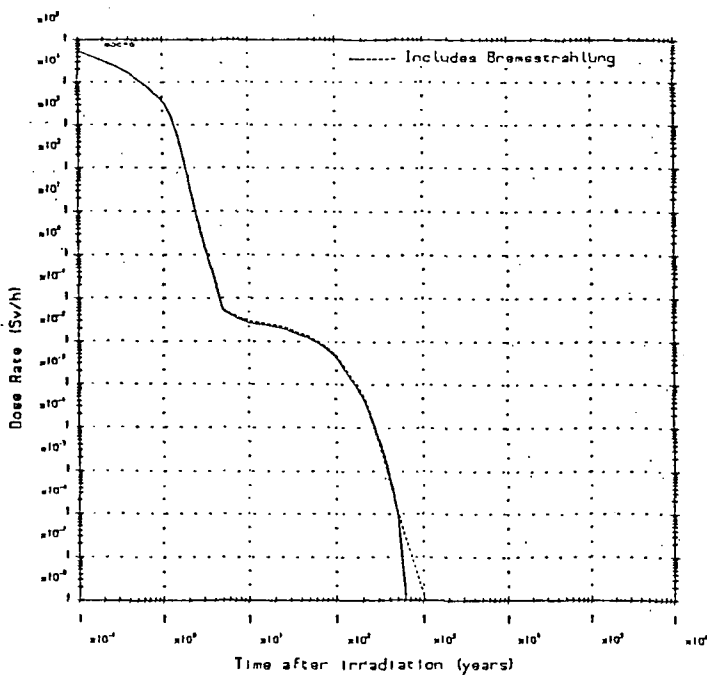
Isotopes	⁴⁶ Ti	⁴⁷ Ti	⁴⁸ Ti	⁴⁹ Ti	⁵⁰ Ti	Atomic Weight = 47.88
Abundance(%)	8.0	7.3	73.8	5.5	5.4	Density = 4.54 Mg m ⁻³



Activity (Bq kg⁻¹) for natural Ti.

Zero time activity:

⁴⁸ Sc(1.820 d)	2.52 10 ¹⁴
⁴⁶ Sc(83.82 d)	1.35 10 ¹⁴
⁴⁷ Sc(3.40 d)	1.31 10 ¹⁴
⁴⁵ Ca(163.0 d)	8.91 10 ¹³
Other nuclides	1.34 10 ¹⁴
Total	7.42 10 ¹⁴



Dose Rate (Sv h⁻¹) for natural Ti.

Zero time dose rate:

⁴⁸ Sc(1.820 d)	2.35 10 ⁵
⁴⁶ Sc(83.82 d)	7.37 10 ⁴
Other nuclides	5.47 10 ³
Total	3.14 10 ⁵

Important long lived nuclides

³⁹Ar(269.0 y), ⁴²Ar(33.0 y), ⁴²K(12.37 h), ⁴¹Ca(1.03 10⁵ y)

Percentage of nuclide from natural abundance of isotope

	⁴⁶ Ti	⁴⁷ Ti	⁴⁸ Ti	⁴⁹ Ti	⁵⁰ Ti
³⁹ Ar	97.06	0.86	2.08	3.35 10 ⁻³	3.54 10 ⁻⁵
⁴² Ar	13.90	0.35	84.65	1.09	5.41 10 ⁻³
⁴¹ Ca	84.45	0.50	15.04	1.14 10 ⁻²	4.45 10 ⁻⁵

Figure 1.14 (continued)

Dominant Reactions

	Reaction	%	F
39Ar			
$^{46}\text{Ti}(n,a)$	$^{43}\text{Ca}(n,na)^{39}\text{Ar}$	80.3	2-2
$^{46}\text{Ti}(n,a)$	$^{43}\text{Ca}(n,2n)^{42}\text{Ca}(n,a)^{39}\text{Ar}$	7.3	3-3
$^{46}\text{Ti}(n,a)$	$^{43}\text{Ca}(n,a)^{40}\text{Ar}(n,2n)^{39}\text{Ar}$	7.4	3-3
$^{47}\text{Ti}(n,a)$	$^{44}\text{Ca}(n,2n)^{43}\text{Ca}(n,na)^{39}\text{Ar}$	29.7	3-3
$^{47}\text{Ti}(n,a)$	$^{44}\text{Ca}(n,na)^{40}\text{Ar}(n,2n)^{39}\text{Ar}$	27.2	3-3
$^{47}\text{Ti}(n,2n)$	$^{46}\text{Ti}(n,a)^{43}\text{Ca}(n,na)^{39}\text{Ar}$	24.9	3-3
$^{48}\text{Ti}(n,a)$	$^{45}\text{Ca}(\beta^-)^{45}\text{Sc}(n,a)^{42}\text{K}(\beta^-)^{42}\text{Ca}(n,a)^{39}\text{Ar}$	96.3	3-3
$^{49}\text{Ti}(n,a)$	$^{46}\text{Ca}(n,a)^{43}\text{Ar}(\beta^-)^{43}\text{K}(\beta^-)^{43}\text{Ca}(n,na)^{39}\text{Ar}$	45.1	3-3
$^{49}\text{Ti}(n,a)$	$^{46}\text{Ca}(n,2n)^{45}\text{Ca}(\beta^-)^{45}\text{Sc}(n,a)^{42}\text{K}(\beta^-)^{42}\text{Ca}(n,a)^{39}\text{Ar}$	22.7	4-4
$^{49}\text{Ti}(n,2n)$	$^{48}\text{Ti}(n,a)^{45}\text{Ca}(\beta^-)^{45}\text{Sc}(n,a)^{42}\text{K}(\beta^-)^{42}\text{Ca}(n,a)^{39}\text{Ar}$	17.3	4-4
$^{50}\text{Ti}(n,a)$	$^{47}\text{Ca}(\beta^-)^{47}\text{Sc}(\beta^-)^{47}\text{Ti}(n,a)^{44}\text{Ca}(n,2n)^{43}\text{Ca}(n,na)^{39}\text{Ar}$	18.7	4-4
$^{50}\text{Ti}(n,a)$	$^{47}\text{Ca}(\beta^-)^{47}\text{Sc}(\beta^-)^{47}\text{Ti}(n,a)^{44}\text{Ca}(n,na)^{40}\text{Ar}(n,2n)^{39}\text{Ar}$	17.1	4-4
$^{50}\text{Ti}(n,2n)$	$^{49}\text{Ti}(n,a)^{46}\text{Ca}(n,a)^{43}\text{Ar}(\beta^-)^{43}\text{K}(\beta^-)^{43}\text{Ca}(n,na)^{39}\text{Ar}$	15.9	4-4
$^{50}\text{Ti}(n,a)$	$^{47}\text{Ca}(\beta^-)^{47}\text{Sc}(\beta^-)^{47}\text{Ti}(n,2n)^{46}\text{Ti}(n,a)^{43}\text{Ca}(n,na)^{39}\text{Ar}$	15.6	4-4
42Ar			
$^{46}\text{Ti}(n,a)$	$^{43}\text{Ca}(n,2p)^{42}\text{Ar}$	87.6	2-2
$^{46}\text{Ti}(n,2p)$	$^{45}\text{Ca}(n,a)^{42}\text{Ar}$	11.2	2-2
$^{47}\text{Ti}(n,2p)$	$^{46}\text{Ca}(n,na)^{42}\text{Ar}$	64.2	2-2
$^{47}\text{Ti}(n,a)$	$^{44}\text{Ca}(n,2n)^{43}\text{Ca}(n,2p)^{42}\text{Ar}$	11.4	3-3
$^{48}\text{Ti}(n,a)$	$^{45}\text{Ca}(n,a)^{42}\text{Ar}$	99.8	2-2
$^{49}\text{Ti}(n,a)$	$^{46}\text{Ca}(n,na)^{42}\text{Ar}$	90.0	2-2
$^{50}\text{Ti}(n,2n)$	$^{49}\text{Ti}(n,a)^{46}\text{Ca}(n,na)^{42}\text{Ar}$	90.1	3-3
41Ca			
$^{46}\text{Ti}(n,a)$	$^{43}\text{Ca}(n,2n)^{42}\text{Ca}(n,2n)^{41}\text{Ca}$	67.6	3-3
$^{46}\text{Ti}(n,d)$	$^{45}\text{Sc}(n,a)^{42}\text{K}(\beta^-)^{42}\text{Ca}(n,2n)^{41}\text{Ca}$	13.2	3-3
$^{46}\text{Ti}(n,d)$	$^{45}\text{mSc}(\text{IT})^{45}\text{Sc}(n,a)^{42}\text{K}(\beta^-)^{42}\text{Ca}(n,2n)^{41}\text{Ca}$	13.2	3-3
$^{47}\text{Ti}(n,a)$	$^{44}\text{Ca}(n,2n)^{43}\text{Ca}(n,2n)^{42}\text{Ca}(n,2n)^{41}\text{Ca}$	27.8	4-4
$^{47}\text{Ti}(n,2n)$	$^{46}\text{Ti}(n,a)^{43}\text{Ca}(n,2n)^{42}\text{Ca}(n,2n)^{41}\text{Ca}$	23.2	4-4
$^{47}\text{Ti}(n,t)$	$^{45}\text{mSc}(\text{IT})^{45}\text{Sc}(n,a)^{42}\text{K}(\beta^-)^{42}\text{Ca}(n,2n)^{41}\text{Ca}$	10.0	3-3
$^{48}\text{Ti}(n,a)$	$^{45}\text{Ca}(\beta^-)^{45}\text{Sc}(n,a)^{42}\text{K}(\beta^-)^{42}\text{Ca}(n,2n)^{41}\text{Ca}$	99.1	3-3
$^{49}\text{Ti}(n,a)$	$^{46}\text{Ca}(n,2n)^{45}\text{Ca}(\beta^-)^{45}\text{Sc}(n,a)^{42}\text{K}(\beta^-)^{42}\text{Ca}(n,2n)^{41}\text{Ca}$	49.9	4-4
$^{49}\text{Ti}(n,2n)$	$^{48}\text{Ti}(n,a)^{45}\text{Ca}(\beta^-)^{45}\text{Sc}(n,a)^{42}\text{K}(\beta^-)^{42}\text{Ca}(n,2n)^{41}\text{Ca}$	38.0	4-4
$^{50}\text{Ti}(n,2n)$	$^{49}\text{Ti}(n,a)^{46}\text{Ca}(n,2n)^{45}\text{Ca}(\beta^-)^{45}\text{Sc}(n,a)^{42}\text{K}(\beta^-)^{42}\text{Ca}(n,2n)^{41}\text{Ca}$	33.8	5-5
$^{50}\text{Ti}(n,2n)$	$^{49}\text{Ti}(n,2n)^{48}\text{Ti}(n,a)^{45}\text{Ca}(\beta^-)^{45}\text{Sc}(n,a)^{42}\text{K}(\beta^-)^{42}\text{Ca}(n,2n)^{41}\text{Ca}$	25.8	5-5

1ppm impurities in iron

Activity (Bq kg^{-1}) @ 50y	$2.72 \cdot 10^2$	@ 100y	$1.00 \cdot 10^2$
Dose Rate (Sv h^{-1}) @ 50y	$1.15 \cdot 10^{-8}$	@ 100y	$4.03 \cdot 10^{-9}$
Limit (100y Dose Rate): 0.62%.			

Heating (W kg^{-1})

Years	0	1	5	10	50	100
Beta	19.5	$3.5 \cdot 10^{-1}$	$5.6 \cdot 10^{-4}$	$8.1 \cdot 10^{-5}$	$3.5 \cdot 10^{-5}$	$1.2 \cdot 10^{-5}$
Gamma	184.6	2.1	$2.8 \cdot 10^{-5}$	$1.4 \cdot 10^{-5}$	$6.2 \cdot 10^{-6}$	$2.2 \cdot 10^{-6}$
Total	204.1	2.5	$5.8 \cdot 10^{-4}$	$9.6 \cdot 10^{-5}$	$4.1 \cdot 10^{-5}$	$1.5 \cdot 10^{-5}$

Minimum Biological Hazard (Sv kg^{-1})

Years	0	1	5	10	50	100
Ingestion	$7.8 \cdot 10^5$	$2.5 \cdot 10^4$	$3.1 \cdot 10^1$	$1.0 \cdot 10^{-1}$	$3.8 \cdot 10^{-2}$	$1.3 \cdot 10^{-2}$
Inhalation	$1.2 \cdot 10^6$	$6.6 \cdot 10^4$	$6.1 \cdot 10^1$	$1.2 \cdot 10^{-1}$	$4.3 \cdot 10^{-2}$	$1.6 \cdot 10^{-2}$

Comments

The bremsstrahlung contribution from ^{42}K is significant (11.7%) over the time scale 5-500 years, while that from ^{39}Ar is dominant at 1000 years.

1.11 Measurement of gamma-ray emission excitation functions in support of JET gamma-ray diagnostics (G. Sadler*, M. J. Loughlin*, J. M. Adams, E. Clipsham*, O. N. Jarvis*, P van Belle* and N. Watkins)

In the JET⁽¹⁾ tokamak the fusion plasmas are created in a large torus-shaped vacuum chamber, and contact between the hot plasma and the walls of the chamber is minimised by confining the conducting plasma within a magnetic field. The plasma, which presently consists of deuterium, is initially heated by passing a large current of approximately 5 MA through it, causing the temperature of the plasma to rise to ~ 3 keV (1 keV \approx 11.6 10^6 K). To achieve temperatures of the order of 10 to 20 keV, which are more appropriate to a thermonuclear reactor, additional heating is required. At JET two major auxiliary heating methods are used. The first involves the injection of up to 20 MW of neutral deuterium atoms at 80 keV per atom (NBI). The second method, Ion Cyclotron Resonance Heating (ICRH), involves launching up to 18 MW of radiofrequency waves into the plasma, and is capable of driving particles into the MeV energy range, thus making it possible to use nuclear techniques to study the effect and effectiveness of this method of heating.

JET plasmas are often contaminated by small amounts of Carbon and Oxygen which originate from the unavoidable contact between the plasma and the wall of the containment vessel. In future, a large part of this wall will be lined with Beryllium so one may reasonably expect small amounts of Beryllium to be present in the plasma as well.

The presence of ICRH-accelerated p, d and ³He ions, as well as contaminants such as C, O and Be, enables the use of γ -spectroscopy to gain information about the fast (ICRH) ion population in the plasma.

* JET Joint Undertaking.

(1) P. H. Rebut and B. E. Keen, Fusion Technology 11 (1987) 13.

Experimental Evidence on JET⁽¹⁾

Figure 1.15 shows an example of a γ -ray spectrum from a well shielded Bismuth Germanate (BGO) scintillator assembly which views the JET plasma through a specially thinned port of the vacuum vessel. The relevant γ -lines have been identified and one can immediately conclude that some deuterium nuclei had energies in excess of the 1 MeV necessary for the 3854 keV γ -line from $^{12}\text{C}(d,p_3)^{13}\text{C}$ to be observable. The use of γ -rays for fusion diagnostic purposes was first proposed by Medley et al⁽²⁾.

Measurements of the excitation functions

The reactions appropriate to this work have been studied in great detail and information is available in the literature. Unfortunately the published information is not always directly applicable to the problems at hand since the excitation functions are normally tabulated in terms of the charged particles emitted at discrete angles. The difficulties and uncertainties in reconstructing the required excitation functions, taking into account γ -ray decay schemes and angular distributions, led us to (re)measure the relevant γ -ray emission excitation functions directly. This work was carried out on the Harwell 5MV Van de Graaff accelerator⁽³⁾ using monoenergetic p, d, ^3He and α ion beams with energies ranging from 500 to 400 keV. The resultant γ -ray spectra were measured simultaneously using two detectors: a germanium solid state detector (HPGe) and 75 mm diameter by 75 mm thick Bismuth Germanate scintillator assembly (BGO). The detectors were positioned close to the target in order to minimise any angular dependence in the γ -emission. A schematic diagram of the detector arrangement is given in Figure 1.16.

-
- (1) G. Sadler, O. N. Jarvis, P. van Belle and J. M. Adams, Europhysics Conference Abstracts, 15th European Conference on Controlled Fusion and Plasma Physics, Dubrovnik, 1988 part 1, p. 131.
 - (2) S. S. Medley, F. E. Cecil, D. Cole, M. A. Conway and F. J. Wilkinson, Rev. Sci. Instr. 56 (1985) 975, and references therein.
 - (3) P. M. Read and J. H. Stevens, Nucl. Instr. and Meth. A249 (1986) p. 141.

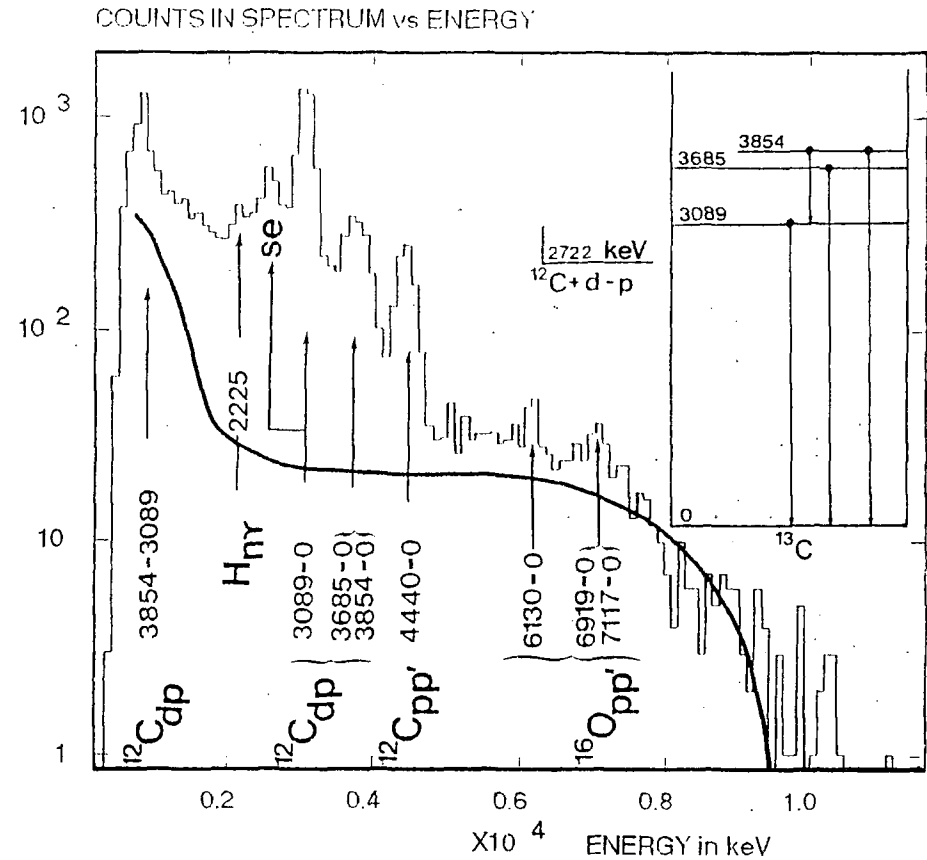
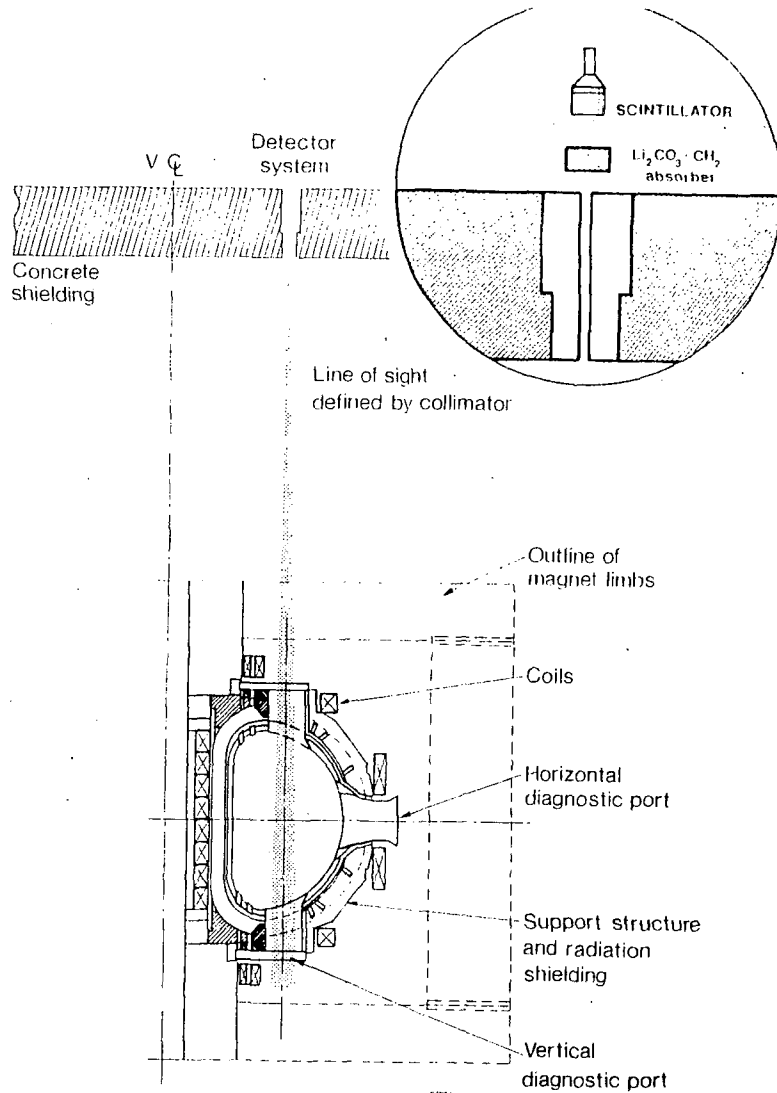


Figure 1.15: a) BGO detector line-of-sight with respect to the JET vacuum vessel.
 b) A typical γ -ray spectrum obtained on JET during combined NBI and ICRH heating (the solid line represents the approximate contribution to the spectrum due to neutral beam injection alone).

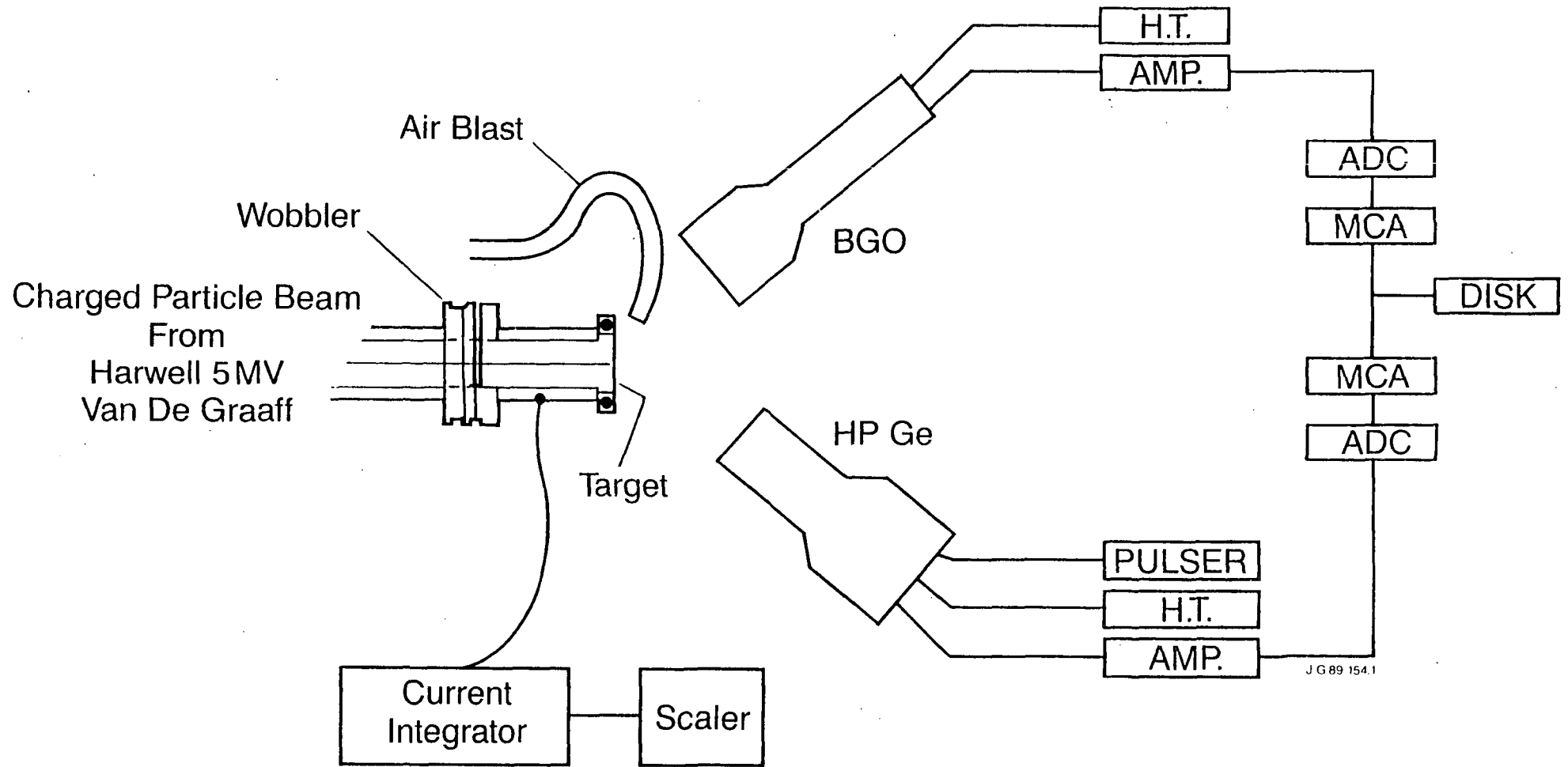


Figure 1.16 A Schematic view of the experimental arrangement.

Table 1.9 lists the various beam-target combinations for which measurements have been obtained. Figures 1.17 and 1.18 show respectively typical examples of γ -ray spectra obtained simultaneously with the (high resolution, low efficiency) HPGe detector and the (low resolution, high efficiency) BGO detector. The energy calibration of the detectors was obtained using standard X-ray sources up to 6.13 MeV.

TABLE 1.9
Summary of measurements

Beam	Target	Energy Range (MeV)	Extent of measurement
p	^9Be	1.0 - 4.0	Several spectra
d	^9Be	0.5 - 4.0	Excitation function
d	C nat	0.5 - 4.0	Excitation function
d	^{13}C	1.0	1 spectrum
d	O nat	0.5 - 4.0	Excitation function
^3He	LiF	4.0	1 spectrum
^3He	^9Be	0.5 - 4.0	Excitation function
^3He	^{10}B	4.0	1 spectrum
^3He	^{11}B	2.0 - 4.0	A few spectra
^3He	C nat	0.5 - 4.0	Excitation function
^3He	^{13}C	0.5 - 1.25	A few spectra
^3He	O nat	4.0	1 spectrum
α	^9Be	0.5 - 4.0	Excitation function

Analysis of the Excitation Functions

A total of 350 such spectra were accumulated in the course of these measurements for the range of ion beam species, target materials and ion beam energies indicated in Table 1.9. The prominent γ -lines, plus those of lesser intensity, were subsequently identified and attributed to the de-excitation of the appropriate excited nuclear state.

The γ -line intensities for each separate beam-target combination were then plotted as a function of incident ion beam energy to produce the final γ -ray emission excitation functions, examples of which are shown in Figures 1.19 and 1.20.

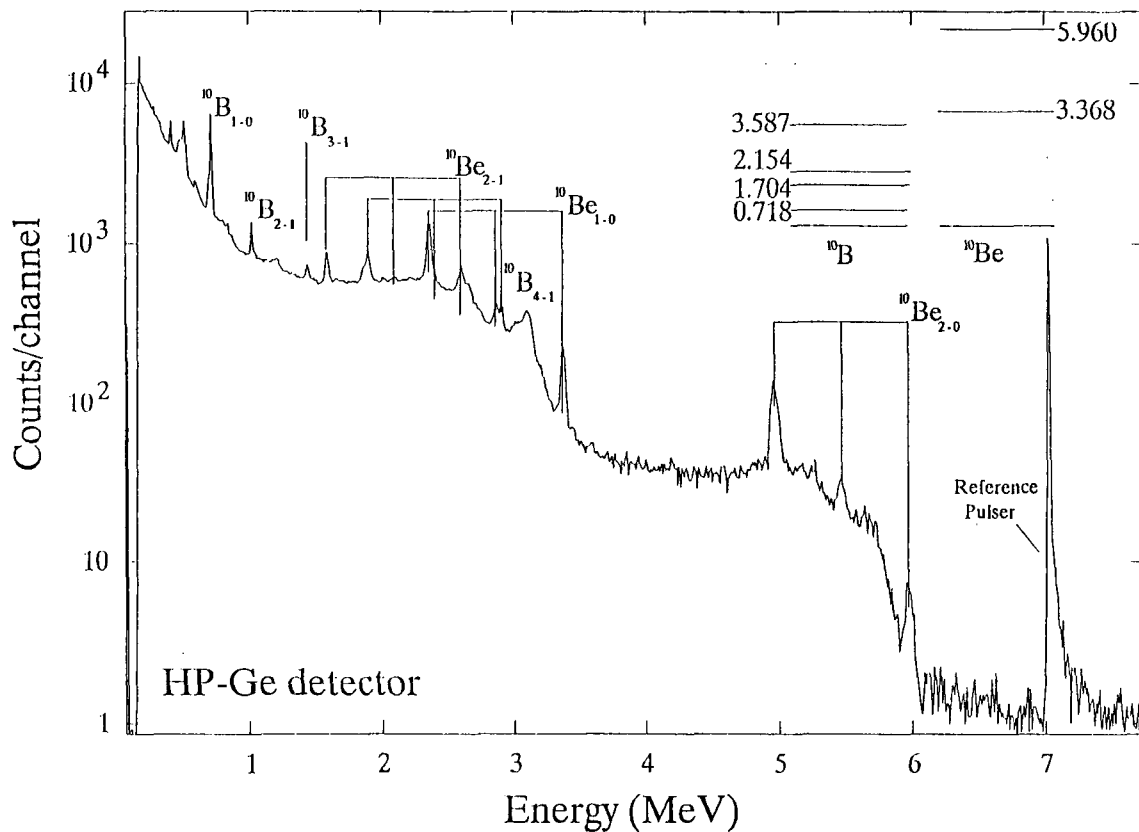


Figure 1.17 Resultant γ -ray spectrum for the bombardment of a 1 mg/cm^2 Be target by 3.5 MeV deuterons (HP Ge detector)

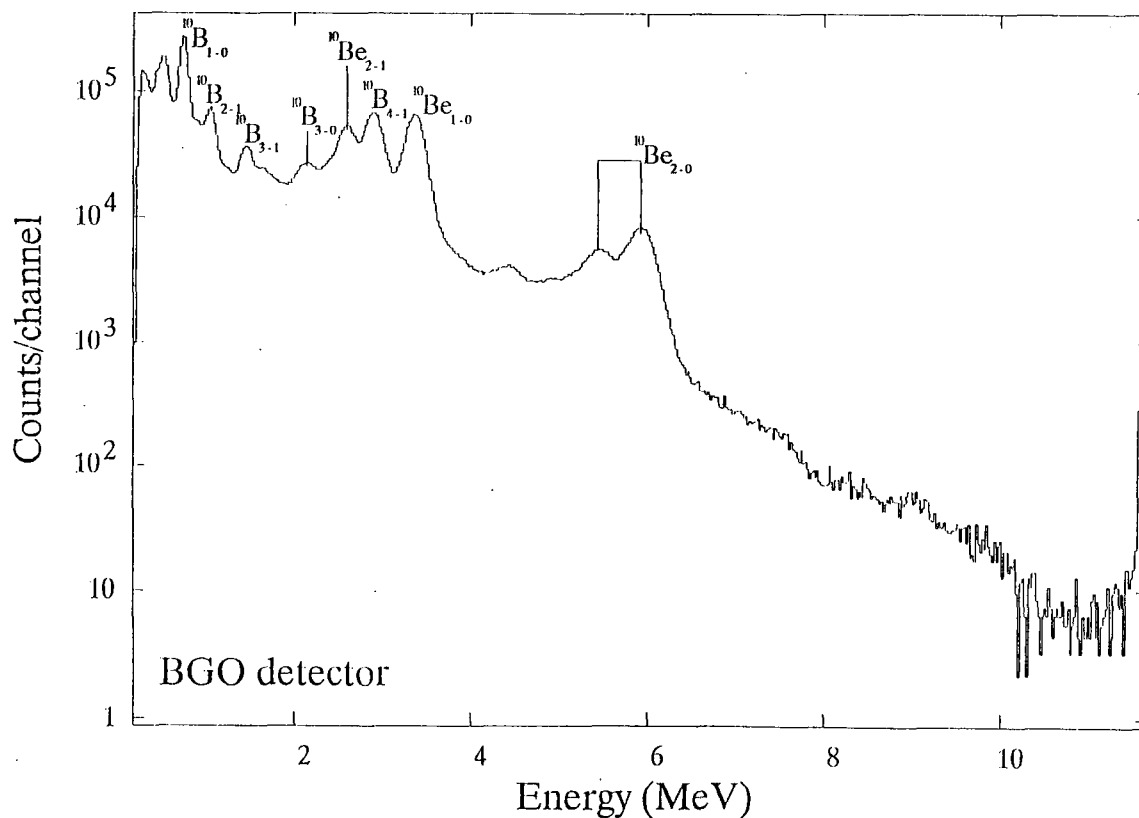


Figure 1.18 As figure 1.17 but with BGO detector

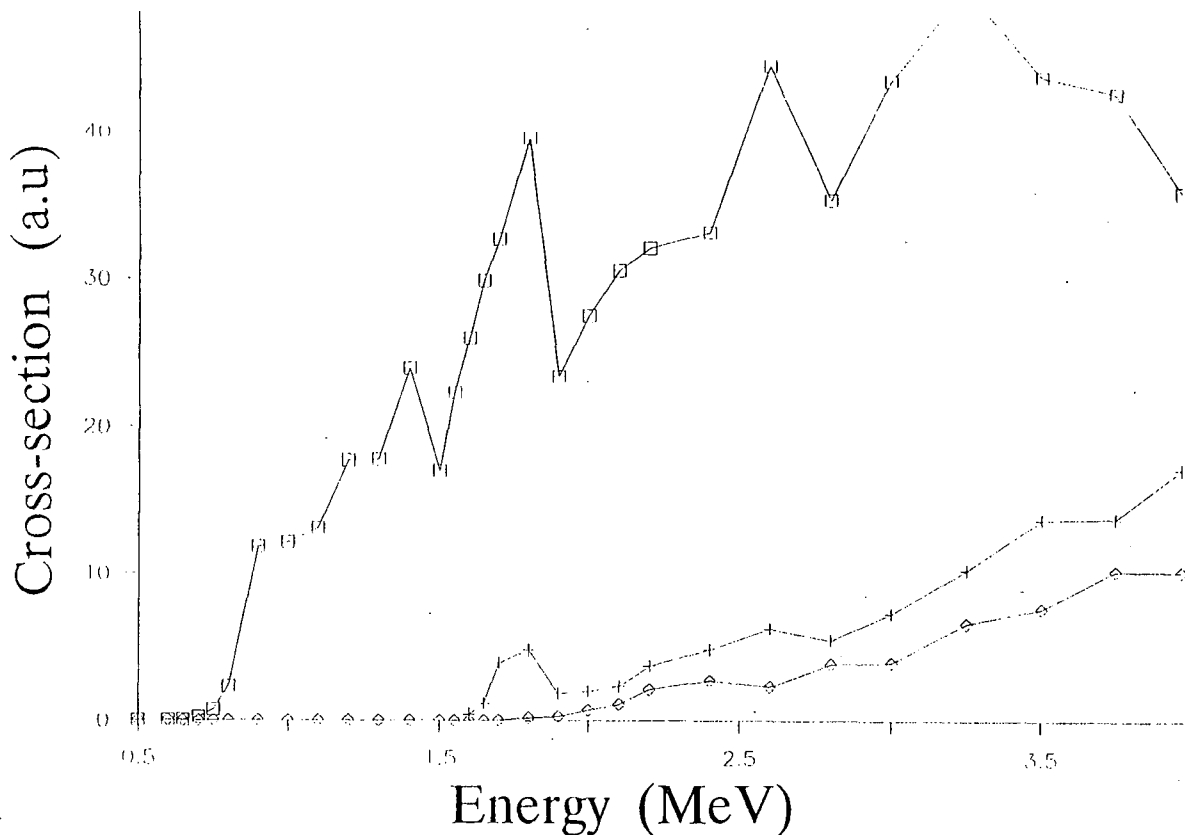


Figure 1.19 Measured γ -emission excitation function for $^{12}\text{C}+d$ as obtained with the HP Ge detector (3.089 MeV level; + 3.685 MeV level and 3.854 MeV level in ^{13}C).

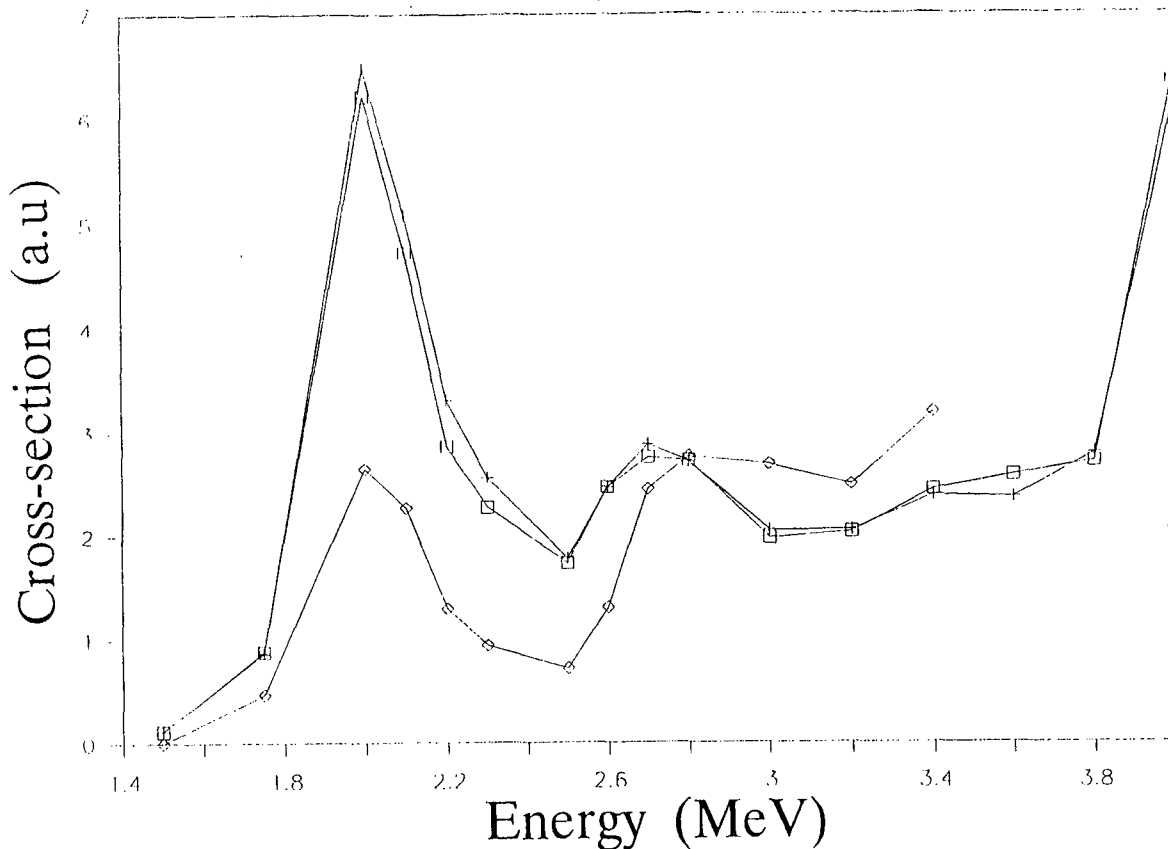


Figure 1.20 $^9\text{Be} + \alpha$ γ -emission excitation function showing excellent agreement between HP Ge and BGO detectors (;+). Also shown for comparison is the $^9\text{Be}(\alpha,n)^{12}\text{C}$ neutron emission function at 0° (J. M. Adams, unpublished) measured on IBIS, the Harwell 3MV pulsed Van de Graaf.

Concluding Remarks

As can be seen from Figure 1.17 some of the γ -lines exhibit significant Doppler shifts and broadening due to the short half-lives of the emitting levels being short compared with the slowing down time in the target of the emitting nucleus. It is interesting to note that in plasmas the thermalisation time of the recoiling ions is always much longer than the decay life-times so all the lines are Doppler shifted. Integration over all angles causes the lines to be broadened.

Conspicuously absent from most of the spectra are lines emanating from pure capture reactions where all the excess energy appears as γ -rays. Such reactions would be useful since the γ -ray energy would be directly related to the energy of the fast particles.

2. CHEMICAL NUCLEAR DATA

(UKCNDC Chairman A. L. Nichols)

2.1 Introduction

Three meetings of the UK Nuclear Data Committee (UKCNDC) (Chairman A. L. Nichols (AEEW) and Secretary P. Robb (AEEW)) were held during 1988 at the beginning of January, July and December. The Data Library Sub-committee (Chairman A. Tobias (CEGB) and Secretary M. F. James (AEEW)) met twice over this same period. Much of the progress during the year has involved the development of techniques to measure tritium yields in ternary fission (Section 2.2.1) and studies identified with alpha and gamma-ray spectroscopy (Section 2.2.4); evaluation efforts have concentrated on fission product yields and considerable progress has been made on the basis of successful collaboration between the University of Birmingham and AEE Winfrith. There has been a new injection of effort into the UKCNDC data evaluation programme, and this should result in progress beyond 1988. Decay data and fission yield evaluations are linked to the establishment of the European Joint Evaluation File (JEF-2). Members of the UKCNDC continue to maintain an influential role in the formulation of JEF-2. Various procedures have been debated and agreed during the year with meetings in Saclay and London. Progress has been slow because of other pressing commitments involving UK evaluators.

Serious cut-backs will occur shortly in direct Government funding for the R&D programmes of the fast reactor and fusion. This will inevitably have a significant impact on a wide range of work within the UKAEA, including the feasibility of achieving and maintaining the facilities to undertake nuclear data measurements and evaluations of interest to the UKCNDC. Such a serious situation is highly regrettable and bodes ill for the immediate future; support for chemical nuclear data stood at between 2½ and 3½ scientist years in the UK during 1988, bolstered by the multi-funded EMR contract on fission yield evaluation with the University of Birmingham. The role of the UKAEA in such work will be seriously challenged by economic problems in the foreseeable future, and the threatened loss of specific laboratories and other expertise would be a major tragedy. Terminal decisions can be expected, and efforts must continue to emphasise the need to undertake data measurements and evaluations for commercial and technical reasons.

2.2 Measurements

2.2.1 Yield of tritium in ternary fission (J. W. Mcmillan and I. G. Jones (Harwell Laboratory))

During the year work was initially concentrated on the reduction of the tritium in the apparatus blank to a low level ca 5 dpm. This was principally achieved by reduction of the hydrogen concentration in the helium carrier gas from 1% to 0.1%, and by preconditioning the gas by scrubbing with low-tritium content water and reducing the water vapour content to a low level by passing through silica gel. While the pick-up of tritium during the subsequent handling of the blanks was shown to be measurable, the amount involved was low relative to other sources.

Recovery experiments have been performed at tritium levels between 20 and 1000 dpm. The results show that recoveries of ca 100% can be achieved. However, blank levels tended to be raised at the end of the high-level experiments, indicating that collection times greater than 3h needed to be adopted.

Prior to separating tritium from the specimens irradiated in ZEBRA, the number of fissions in each sample was determined non-destructively by gamma-ray spectroscopy. The ^{137}Cs content was measured in each capsule, and the inherent activity of the uranium or plutonium was used to calibrate the measurements. The determined fissions ranged between ca 5 and 7×10^{13} , equivalent to several hundred dpm of tritium. A number of disturbing results have been encountered during trials of the separation method on unirradiated specimens of uranium and plutonium, and during the determination of tritium in 2 of the 6 empty aluminium capsules irradiated in ZEBRA. While specimens of uranium and plutonium, both with aluminium, were successfully melted in the separation apparatus, significant amounts of tritium (350 to 450 dpm g^{-1}) were recovered. The source of tritium was not the aluminium, and although the materials employed were not those utilised for the ZEBRA experiments, extraneous tritium may have been present in the uranium and plutonium specimens which were irradiated. Concern has always existed regarding the presence of tritium producing nuclides (eg ^6Li , and ^{10}B) in the aluminium used for the irradiation capsules. While the tritium found in the first irradiated capsule was < 25 dpm, the tritium in the second irradiated capsule was ca 155 dpm, a highly significant quantity. Final judgement on the overall significance of these results must await analysis of the 4 remaining blank capsules.

2.2.2 Absolute fission yields of selected fission products
(T. W. Kyffin (DNPDE))

The aim is to measure the fission yields on Nd nuclides, $^{95}\text{Nb}/^{95}\text{Zr}$, ^{106}Ru , ^{137}Cs and ^{144}Ce in high burn-up samples of ^{235}U , ^{238}U , ^{239}Pu , ^{240}Pu and ^{241}Pu . The pins containing the fission yield samples have been pulled from the sub-assembly and the individual pinlets recovered. Of the 12 pinlets irradiated, two failed completely (one ^{239}Pu sample and the ^{240}Pu specimen), and two have lost their fission gas but the fuel remains intact (both ^{238}U). The remaining three ^{235}U , two ^{239}Pu , one ^{241}Pu and two dummy pinlets are complete and are now stored in the analytical facilities at DNPDE awaiting a final decision on funding.

A proposal has been formulated in the hope of obtaining support from the UKAEA underlying research budget. Other sources of funding are also being sought outside the UKAEA.

2.2.3 Measurements of alpha in PFR (A. Tyrrell and P. Thompson (AWE))

Results for the final sample (RST 28/42) are reported in Table 2.1. Other pressures have precluded further work this year, although it is still intended to undertake alpha-particle spectrometry on ^{241}Am , to provide $^{238}\text{Pu}/^{239}\text{Pu}$ ratios, and prepare a final report of this collaborative work.

TABLE 2.1

Sample	^{242}Pu	
Dounreay	RST 28/42	
AWE	542 42	
Zero Time	18.8.79	
Nuclide	Atoms	% rsd
^{239}Pu	1.745×10^{13}	1.254
^{240}Pu	2.677×10^{13}	1.331
^{241}Pu	5.06×10^{12}	6.323
^{242}Pu	1.650×10^{15}	1.006
^{60}Co	1.481×10^{10}	6.494
^{125}Sb	2.488×10^{10}	16.52
^{134}Cs	3.810×10^{10}	1.190
^{137}Cs	3.008×10^{12}	0.460
^{144}Ce	9.375×10^{11}	5.953
^{154}Eu	2.471×10^{10}	6.169
^{155}Eu	2.134×10^{11}	2.897
^{241}Am	5.761×10^{12}	1.198
^{243}Am	4.218×10^{13}	0.591
^{243}Cm	2.153×10^{10}	65.55

2.2.4 Measurement of radionuclide decay data (M. F. Banham, A. J. Fudge, R. McCrohon, G. Raw, R. A. P. Wiltshire and I. Jackson (Harwell Laboratory))

Efforts have continued to improve the measurement facilities which include a full range of alpha-particle and gamma-ray counting and spectroscopy systems. Accreditation of the laboratory under the National Physical Laboratory NAMAS scheme is being sought for measurements of alpha-particle emitters. Although gamma-ray measurements are not being included in this scheme, some gamma-ray spectrometers are now subject to strict quality control procedures.

Work has continued in the following areas:

- (a) Measurement of ^{93m}Nb : Development of methods for measuring the low energy emissions has continued, and high resolution x-ray spectroscopy and liquid scintillation counting are now used routinely. The use of a thin caesium iodide crystal as an intermediate system has been investigated. This provides modest resolution and a sensitivity about 10 times greater than the high resolution counting, with the advantage over liquid scintillators of simpler source preparation. It is proposed to prepare a standardized solution of ^{93m}Nb from a well-characterised high-purity and high specific activity source.
- (b) Plutonium fast fission yield of ^{129}I : Work continues on the measurement of the fast fission yield of ^{129}I from ^{239}Pu .
- (c) International exercise for P_γ measurements of ^{75}Se : Measurements were completed and forwarded to the co-ordinator of this exercise for evaluation. The relative intensities are listed in Table 2.2.

TABLE 2.2

Relative Gamma-ray Emission Probabilities of ^{75}Se

Energy (keV)	Relative Emission Probabilities	Relative Standard Deviation
66.06	1.863	0.68
96.73	5.765	0.35
121.12	28.978	0.37
136.00	100.000	0.20
198.60	2.556	0.40
264.66	98.857	0.14
279.54	41.767	0.10
303.92	2.193	0.38
400.66	19.139	0.13
419.0	0.024	5.62
572.5	0.066	3.10
617.6	0.011	11.30

- (d) Preparation of sources for nuclear data measurements:
Sources have been prepared of ^{236}Pu , ^{227}Ac , and ^{232}U for use in other laboratories.
- (e) Decay scheme of ^{237}Np : Following the successful analysis of the alpha spectrum by Bortels et al at Geel(1), attempts are being made to evaluate the decay scheme.
- (f) Decay scheme of ^{239}Np : Measurements of half-life, P_x and P_γ are being carried out by a CASE award student at Imperial College, London, funded and partly supervised by Chemistry Division, Harwell Laboratory.

2.2.5 Measurement and evaluation of half-lives and gamma-ray emission probabilities (I. M. Lowles, T. D. McMahon and M. U. Rajput (Imperial College Reactor Centre, Ascot))

- (a) Measurements of P_γ in ^{65}Ni , ^{125}Sb and $^{239}\text{U}/^{239}\text{Np}$ have continued in 1988. The P_γ studies of ^{65}Ni have been completed.
- (b) Half-life data for ^{90}Sr , ^{137}Cs and ^{252}Cf have been re-evaluated and published as a UKCNDP paper (CNDP(88)P28). Recommended half-lives are:

^{90}Sr	28.67	\pm 0.18	y
^{137}Cs	30.11	\pm 0.08	y
^{252}Cf	2.651	\pm 0.002	y

- (c) Attempts are being made to reconcile recently reported α , γ and conversion electron measurements in the decay of ^{237}Np .

2.3 CNDP Data Library Sub-Committee

Membership during 1988:	A. Tobias	CEGB, BNL (Chairman)
	M. F. James	AEEW (Secretary)
	A. J. Fudge	Harwell Laboratory
	R. W. Mills	University of Birmingham
	P. Robb	AEEW
	D. R. Weaver	University of Birmingham
	A. Whittaker	BNF plc

(1) G. Bortels, D. Mouchel and R. Eykens, Annual Progress Report on Nuclear Data 1987, CBNM, Geel, Belgium, October 1988.

2.3.1 Data library development

The current status of the UKCNDC Data Libraries is summarised in Table 2.3. While there has been some progress in the evaluation of data for individual nuclides, these results have yet to be incorporated into the UKCNDC data files. In the meantime the JEF-1 decay data and fission yield data files have been endorsed for use in the UK. All UKCNDC evaluations are to be made available for JEF-2.

(a) Heavy Element Decay Data (A L Nichols (AEEW))

Efforts have concentrated on the evaluation of the decay data for the 4n decay chain of $^{236}\text{Np}/^{232}\text{U}$. This work has been completed and efforts are in hand to prepare a report of the various problems experienced during the exercise and the areas of continued uncertainty. These nuclides include:

$^{236\text{m,g}}\text{Np}$, ^{236}Pu , ^{232}U , ^{228}Th , ^{224}Ra , ^{220}Rn , ^{216}Po ,
 ^{212}Pb , $^{212\text{m,n,g}}\text{Bi}$, $^{212\text{m,n,g}}\text{Po}$ and ^{208}Tl

(b) Fission Product Decay Data (A Tobias (CEGB, BNL) and P Robb (AEEW))

No progress has been made on the fission-product decay data files due to lack of resources. However, there has been some involvement with the JEF working group in assessing the improvements to be made for JEF-2.

(c) Activation Product Decay Data (A L Nichols and P Robb (AEEW))

Decay data have been re-evaluated for $^{243}\text{Am}/^{239}\text{Np}$ to assist in the formulation of suitable parameters for the IAEA-CRP on X- and Gamma-ray Standards for Detector efficiency Calibration.

(d) Fission Yields (R W Mills and D R Weaver (University of Birmingham), and M F James (AEEW))

A new evaluation of fission product yields is being produced for the UKFY2 data library, due to be completed early 1989. The evaluation consists of three components as described in detail below.

TABLE 2.3

UK Chemical Nuclear Data Libraries Status Table, December 1988

Data	Present Status	File Development
1 Fission Product Data	Exists as UKFPDD-2 (ENDF/B-IV format) - replaces UKFPDD-1 Total no of nuclides = 855 Radioactive nuclides = 736 Ground state = 175 1st excited state = 133 2nd excited state = 5 Nuclides with spectra = 390 Total no of gamma lines = 11,978 Total no of beta- lines = 3,592 Total no of beta+ lines = 91	Robb (AEEW) evaluating ^{155}Eu , ^{152}Eu , ^{151}Sm , ^{134}Cs , ^{129}Sb and ^{125}Sb . P_n values for delayed neutron precursors from Swedish evaluation. Delayed neutron precursor spectra will possibly be obtained from USENDF/B-VI
2 Activation Product Decay Data	Available in ENDF/B-IV and V format for 91 nuclides as UKPADD-1. Now includes detailed K X-ray spectra.	60 nuclides have been evaluated for UKPADD-2, 56 are in ENDF/B-V format. ^{51}Cr , ^{65}Zn , ^{75}Se and ^{198}Au have been re-evaluated as part of an IAEA programme, and are available in ENDF/B-V format.
3 Heavy Element Actinide Decay Data	Completion of UKHEDD-1, including spontaneous fission data in June 1982. Data in ENDF/B-V format for: Total no nuclides = 125 Ground state = 111 1st metastable state = 13 2nd metastable state = 1 Total no of alpha lines = 767 Total no of beta- lines = 527 Total no of beta+ lines = 39 Total no of gamma lines = 3,475 Total no of discrete electrons = 6,755 Total no of x-rays = 381	^{236}Np , ^{236m}Np , ^{236}Pu , ^{232}U , ^{228}Th , ^{224}Ra , ^{220}Rn , ^{216}Po , ^{212}Pb , ^{212}Bi , ^{212m}Bi , $^{212}\text{m}\text{Bi}$, ^{212}Po , ^{212m}Po , $^{212}\text{m}\text{Po}$ and ^{208}Tl evaluations completed. Evaluation of ^{243}Am is underway ^{231}Pa , ^{234}U and ^{235}U decay data ^{242m}Am and half-life have been evaluated.
4 Fission Yields	Available in ENDF/B-V format based on Banai/James revision. Complete library called UKFY1 UKIFYU1 - unadjusted independent yields UKIFYA1 - adjusted independent yields UKCFYA1 - adjusted cumulative yields	New evaluation underway. Database extended and up-to-date. Initial chain yield evaluation complete: independent and cumulative yields being fitted.

- (i) Spectral Data from the decay data files may be accessed via the retrieval system described by Tobias (RD/B/5170N81, 1981).
- (ii) Much of the decay data and the fission yields from these files have been incorporated in JEF1 data library.

- (i) production of a database of fission product yields;
- (ii) checking for consistency of values within the database;
- (iii) production and use of programs to produce the ENDF/B-VI formatted independent yield libraries (unadjusted and adjusted for physical constraints).

A data base in a new format has been produced, using the data from the earlier database used for the UKFY1 evaluation, data from the EXFOR fission yield library, and new papers found in a literature search. The database now contains all the UKFY1 data; however, the EXFOR library and 'new-paper' data contain only 'useful data'. Data were of no use to the evaluation if they referred to photofission, as there is no plan to include parameters in the UKFY2 database. The numbers of data points from these sources within the fission yield database (version 1.7) are listed in Table 2.4.

TABLE 2.4
Data Points Used in Version 1.7 of UKFY2

	Chain	Fract. Ind.	Fract. Cum.	Cumulative	Independent
UKFY1	1207	494	200	4646	298
EXFOR	912	715	116	1765	702
New papers	25	28	10	158	15
Total	2144	1237	326	6569	1015
%(EXFOR+New)	43.7	60.0	38.7	29.3	70.6

(Percentage EXFOR and new data in new database = 39.4%)

Yields of fission fragments were not used unless several fragment energies were summed and delayed neutron effects removed. As gaps in the measured data will be filled by programs used in the evaluation, only measured yields have been contained within the database. It is intended to include a second database in the evaluation that consists of ratios of yields,

which will be added after an initial evaluation gives a 'best' estimate of the denominator, thus allowing the numerator and its error to be calculated.

The database has been checked from the output of pre-processing programs, which produced tables of evaluated but unadjusted independent, cumulative and chain yields. To stop repeated addition of error due to conversion of fractional to absolute yields (and vice-versa) both fractional and absolute values were converted once, and further processing will only involve the appropriate set of data. The secondary (pre-processed) databases contained weighted means and recommended errors (greater of internal and external errors) for the measured yields.

The checking of the database will be a continuing process, which will initially concentrate on the systems being included in the UKFY2 evaluation. An automatic method of altering the weight of individual datapoints far from the mean value has been used where there was no obvious error or insufficient time to check each discrepant data point in detail. The systems included in the UKFY2 evaluation are:

Thermal: $^{233},^{235}\text{U}$ and $^{239},^{241}\text{Pu}$.

Fast: ^{232}Th , $^{233},^{235},^{238}\text{U}$, ^{237}Np and
 $^{239},^{240},^{241},^{242}\text{Pu}$.

High: ^{232}Th and $^{233},^{235},^{238}\text{U}$.

However, it may be possible to include extra systems if they are required.

Fitting procedures have been used to produce estimates of unmeasured yields. Several techniques have been tried to fit chain yields using a five Gaussian model which gives a reasonable fit to the data. Independent and cumulative yields have been used to calculate \bar{z}_p , σ and the odd-even coefficient C, using \bar{z}_p model of Wahl. When the databases of measured yields are complete, with gaps filled by the above models or similar, the data will be converted into ENDF/B-VI format to produce unadjusted and adjusted libraries. The work should be completed in early 1989.

(e) **Delayed Neutron Data** (M F James (AEEW) and D R Weaver
(University of Birmingham))

A review of delayed neutron data for important fissioning nuclides is in progress as part of the collaboration for the JEF-2 project. The recent Swedish evaluation is recommended as the source of data for P_n values for individual delayed neutron precursors⁽¹⁾.

2.3.2 Joint evaluated file, JEF (P Robb (AEEW))

Work is proceeding with the production and selection of data to be included in JEF-2 which will be constructed in ENDF/B-VI format. Comparisons have been made of the data found in JEF-1 and in other databases to determine whether automatic methods can be employed to include additional data. A number of problems have been highlighted and a critical review is required before automatically selected data can be adopted. Other suitable data include mean decay energy measurements carried out at Studsvik and theoretical values from the Max-Planck Institute. Delayed neutron data recommended by Lund and Rudstam are to be included and these may be supplemented by other experimental and theoretical data if available. All evaluations for inclusion in JEF-2 should be finalised by April 1989.

There is a need for more JEF decay data to be used in fusion reactor materials activation studies, with an outstanding requirement for evaluated data describing 100 nuclides.

(1) E Lund, G Rudstam, et al. A Status Report on Delayed Neutron Branching Ratios of Fission Products, Proc. of Specialists' Meeting on Delayed Neutron Properties, University of Birmingham, September 1986, (ISBN 07044 0926 7); and G Rudstam, private communication, 1988

3. DIVISION OF RADIATION SCIENCE AND ACOUSTICS,
NATIONAL PHYSICAL LABORATORY
Superintendent: Dr A. R. Cox

(Radioactivity and Neutron Measurements Branch)
(Branch Head: Dr P. Christmas)

3.1 International intercomparisons (under the auspices of the International Bureau of Weights and Measures (BIPM))

3.1.1 Radioactivity measurements (D. Smith, M. J. Woods)

The NPL measurement of the activity of ^{125}I by 4π β - γ coincidence counting has been completed. The results have been submitted to BIPM.

3.2 Neutron cross-sections (T. B. Ryves, P. Kolkowski)

The $^{24}\text{Mg}(n,p)^{24}\text{Na}$ reaction cross section at 14 MeV has been measured as a function of foil thickness (see figure 3.1). The observed variation, due to the escape of ^{24}Na ion recoils from the foil during the neutron bombardment, has been accurately predicted by Monte Carlo calculations which utilise the range-energy data of Northcliffe and Schilling. This effect, which can be serious for foil thicknesses required for the highest beta counting efficiencies and some types of reaction involving low-A nuclei, has not been considered before in detail.

In collaboration with the radioactivity measurements group, measurements have been made on the 14 MeV reaction cross sections of $^{165}\text{Ho}(n,p)$ and (n,a) , $^{204}\text{Pb}(n,n')$ and $(n,2n)$ $^{208}\text{Pb}(n,p)$ and $^{209}\text{Bi}(n,p)$ and (n,a) . The much improved accuracies of these results compared with those of earlier published values should help resolve major discrepancies in the systematics of neutron-induced threshold reactions. For example, the NPL value for the $^{165}\text{Ho}(n,p)$ reaction, which is lower than the only other measurement by a factor of ten, is in line with the predicted value.

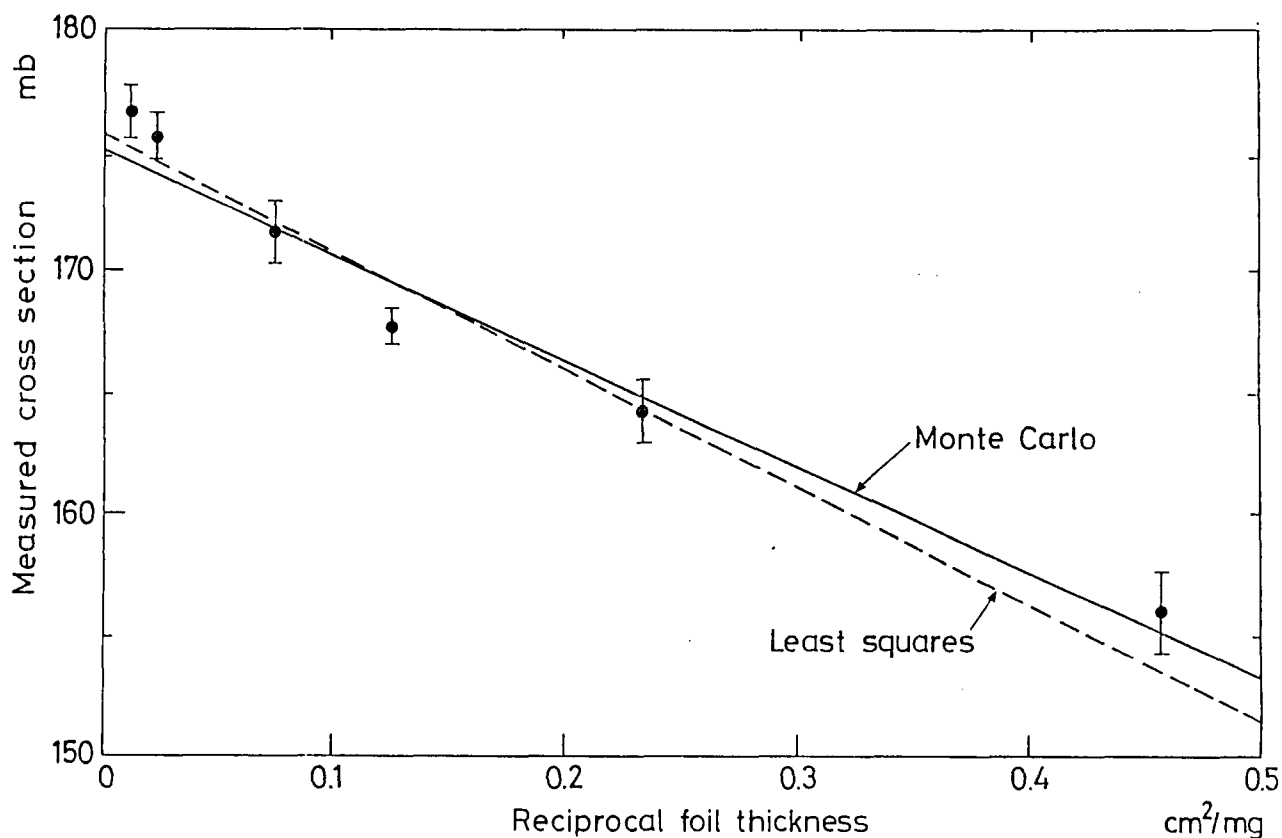


Figure 3.1 The measured cross section at 14.7 MeV for the $^{24}\text{Mg}(n,p)^{24}\text{Na}$ reaction as a function of reciprocal foil thickness, showing a least squares straight line fit and a Monte Carlo calculation.

3.3 Decay data (P. Christmas, D. Smith, S. A. Woods, C. W. A. Downey, W. R. Phillips, J. N. Mo*, J. Pearcey*)

^{201}Tl As part of an international intercomparison to resolve a discrepancy in activity measurements, the γ -ray emission probabilities and half-life have been determined. The results have been submitted for publication.

^{124}I Recent improvements in production techniques allow ^{124}I to be used for positron emission tomography. In collaboration with Manchester University, measurements to determine decay scheme parameters and the half-life have been completed. The results will be presented at the 1989 ICRM meeting.

* Schuster laboratory, University of Manchester, UK.

[1] S. A. Woods, P. Christmas, P. Cross, S. M. Judge and W. Gellately, Nucl. Instr. and Meth. In Phys. Res. A264 (1988) 333, erratum: *ibid*, A270 (1988) 203, addendum: *ibid* A272 (1988) 924.

$^{237}\text{Np}/^{233}\text{Pa}$ The internal conversion coefficients in the energy range 20-300 keV have been published. Measurements of the low energy internal conversion electron spectrum (<20 keV) are to be submitted for publication.

$^{241}\text{Am}/^{244}\text{Cm}$ As part of the SERC-supported collaboration with Manchester University, measurements of the internal conversion electron spectra for these nuclides have been completed. It is intended to publish the results.

^{56}Co Under the auspices of EUROMET, and arising from the IAEA Co-ordinated Research Programme on decay data for selected nuclides for the calibration of γ -ray detectors, studies are being made of ^{56}Co . Material from SCK/CEN (Belgium) has been distributed to NPL, PTB (FRG), and LMRI (France) for the determination of the half-life, and to NPL and PTB for standardisation.

3.4 Evaluations (P. Christmas, M. J. Woods, A. S. Munster)

The final report on the evaluation of half-life data for 33 radionuclides, carried out jointly by NPL and PTB within the framework of an IAEA Co-ordinated Research Programme, is to be presented to the IAEA in June 1989. NPL is continuing this exercise for a large number of other radionuclides.

4. NUCLEAR PHYSICS LABORATORY, UNIVERSITY OF OXFORD

4.1 The unification of the nucleon optical potential

(P. E. Hodgson and Su Zong Di*)

The nuclear mean field has been defined for bound and scattering states and its parameters have been shown to vary continuously over the whole energy range. The real and imaginary parts of the potential have been connected by dispersion relations, unifying the potential from negative to positive energies. The dispersion relations have recently been used to analyse the total cross-sections for the interactions of neutrons with nuclei around 1 MeV. These are generally rather larger than the values given by global neutron optical potentials, and fits with potentials of standard form can only be obtained with rather unphysical values of the parameters. We have applied the dispersion relations to analyse these data, and find that after including the dispersion term in the real potential the data can be fitted without unphysical parameters.

4.2 Multistep analysis of neutron and proton induced reactions below 20 MeV

(M. Chadwick, P. E. Hodgson, R. Bonetti** and A. Marcinkowski)

The quantum mechanical nuclear reaction theory of Feshbach, Kerman and Koonin has been used to analyse multistep compound reactions for a large range of target nuclei and incident energies. A number of improvements have been made to the way in which the theoretical predictions are evaluated. When calculating transition matrix elements, realistic nuclear single particle wavefunctions have been used, unlike Feshbach's original formulation where the wavefunctions were taken to be constant within the nucleus. The distinguishability of neutrons and protons in the nuclear cascade was also investigated, and it was found that to first order this effect could be accounted for by applying correction factors to the original theoretical expressions for the emission rates. This allowed simultaneous fits of (n,p) and (n,n) reaction cross sections for a given target nucleus. The successful analysis, with the reformulated model, of multistep compound emission spectra for (n,n'), (n,p) and (p,n) reactions for incident energies from 9 to 18 MeV has enabled the strength of the residual interaction to be determined, and it was found to be rather constant for different nuclei

* Institute of Atomic Energy, Beijing, China.

** University of Milan, Italy.

and different excitation energies. There is evidence to suggest that in nuclear reactions gamma rays are sometimes emitted before equilibrium is attained, resulting in a large cross section for high energy gamma rays. The theoretical mechanism for pre-equilibrium gamma emission is being developed so that these processes can also be included into the multistep formalism.

A particular application of the modified theory has been in calculating the escape and damping pre-equilibrium widths and the cross section for the ^{107}Ag (n,p) reaction. The results of this work were compared with those obtained using the original Feshbach formulation.

4.3 Neutron emission cross sections on ^{184}W at 11.5 MeV and 26.0 MeV and the neutron - nucleus scattering mechanism (A. Marcinkowski, R. W. Findlay*, J. Rapaport*, P. E. Hodgson and M. B. Chadwick)

Inelastic neutron emission for 11.5 MeV and 26 MeV incident neutron energies has been studied for monoisotopic samples of ^{184}W . Time-of-flight spectra were taken at several angles between 12° and 160° using the beam swinger spectrometer at Ohio University. The data are averaged over 1 MeV energy bins and compared with the quantum-mechanical statistical multistep calculations.

4.4 Work on nuclear model codes

4.4.1 International nuclear model code intercomparison (Su Zong Di** and P. E. Hodgson)

Participation in the International Code Intercomparison organised by the NEA Data Bank in Paris.

The comparison between Chinese unified program (MUP2) and some international nuclear model programs, SMOG, JIB and WILMORE6, has been completed. The results from the different codes show that the accuracy of MUP2 is comparable with the presently attainable accuracy of international nuclear model codes on optical model calculations and Hauser-Feshbach theory calculations. A report has been finished and submitted to the International Atomic Energy Agency, NEA Data Bank and the Chinese Nuclear Data Centre.

* Ohio University, Athens, Ohio, USA

** Institute of Atomic Energy, Beijing, China.

4.4.2 Weisskopf-Ewing and Hauser-Feshbach international nuclear model code intercomparison. (E. Satorit and P. E. Hodgson)

The first results of this intercomparison have been received and are being analysed.

4.5 Nuclear momentum distributions (I.Zh. Petkov, A. N. Antonov and P. E. Hodgson)

The momentum distributions of nucleons in nuclei are being studied using the flucton and single-particle potential models. The flucton model has now been extended to enable the single-particle wavefunctions and occupation numbers to be calculated. A paper is being prepared for publication, giving the results for ^{16}O , ^{40}Ca and ^{208}Pb .

The flucton model is being further extended to calculate the momentum distributions of alpha-particle sub-structures in the nucleus, and these will be used to calculate the cross-sections of some alpha-emitting reactions for comparison with experimental data.

4.6 Nucleon-alpha reactions in nuclei (E. Gadioli* and P. E. Hodgson)

The experimental data on nucleon-alpha reactions to discrete and continuum states have been reviewed, together with the theories that have been proposed to account for them. At low energies the compound nucleus mechanism predominates, and as the energy increases the pre-equilibrium and direct processes become more likely. The results of typical calculations have been compared with the experimental data. Particular attention has been devoted to J-dependent and spectator effects, and to the competition between the triton pick-up and alpha knockout mechanisms.

* University of Milan, Italy.

4.7 Recent publications

The following publications contain more details of the above work carried out in the Nuclear Physics Laboratory at Oxford.

1. Neutron Scattering and Reactions
P. E. Hodgson, J. Phys. G14, 485, 1988.
2. Nuclear Reactions, P. E. Hodgson, A course of eight lectures given at the International centre for Theoretical Physics, Trieste in March 1988, SMR/284-5.
3. Multistep Processes in Nuclear Reactions, P. E. Hodgson, Journal of Scientific Research, Banaras Hindu University, 37, 11, 1987.
4. Comparison between Chinese Unified Program (MUP2) and International Nuclear Model Programs, Su Zong Di and P. E. Hodgson, International Atomic Energy Agency Report INDC (CPR)-012/G + CJ, 1988.
5. Multistep Compound Reactions, P. E. Hodgson and M. B. Chadwick. Proceedings of the Specialists' Meeting on Pre-Equilibrium Nuclear Reactions, Semmering, Austria, 221, 1988.
6. Multistep Processes in Neutron-Induced Reactions, P. E. Hodgson, Proceedings of the 1987 Kiev Conference, Vol. 2, 76, 1988.
7. Angular Momentum in Multistep Compound Processes, M. P. Chadwick, P. E. Hodgson and A. Marcinkowski, Proceedings of the Fifth International Conference on Nuclear Reaction Mechanisms, Ed. E. Gadioli, Varenna, June 1988, Ricerca Scientifica ed Educazione Permanents, Supplemento 66, 102, 1988.
8. Pre-Equilibrium Processes in Nuclear Reactions Intercomparison of Theories and Codes, P. E. Hodgson, Proceedings of the International Conference on Nuclear Data for Science and Technology, MAS, Japan, May 30 -- June 3, 1988, Ed. S. Igarasi, Japan Atomic Energy Research Institute, Saikon Publishing Co. Ltd., 655, 1988.
9. Dispersion Relation Analysis of the Total Neutron Cross-section Anomaly, Su Zong Di and P. E. Hodgson, J. Phys. G14, 1485, 1988.
10. Summary of the Advisory Group Meeting on Nuclear Theory for Fast Neutron Nuclear Data Evaluation, P. E. Hodgson, Beijing, 12-16 October 1987.
11. The Neutron Optical Model Potential, P. E. Hodgson, Proceedings of Advisory Group Meeting on Nuclear Theory for Fast Neutron Nuclear Data Evaluation, Beijing, 12-16 October 1987, IAEA-TECDOC-483, 51, 1988.
12. Multistep Processes in Nuclear Reactions, P. E. Hodgson, Proceedings for an Advisory Group Meeting on Nuclear Theory for Fast Neutron Nuclear Data Evaluation, Beijing, 12-16 October 1987, IAEA-TECDOC-483, 215, 1988.

13. Intercomparison of Nuclear Model Computer Codes, P. E. Hodgson, Proceedings of an Advisory Group Meeting on Nuclear Theory for Fast Neutron Nuclear Data Evaluation, Beijing, 12-16 October 1987, IAEA-TECDOC-483, 309, 1988.
14. Preliminary Analysis of Neutron Optical Potential for $A = 40-60$ below 10 MeV, Su Zong Di, INDC(CPR)-013/LI (INT(88)-1), IAEA, 1988.
15. Theoretical Aspects of Clustering in Nuclei, P. E. Hodgson. Proceedings of the Fifth International Conference on Clustering Aspects in Nuclear and Subnuclear Systems, Kyoto, Japan, Physical Society of Japan, 755, 1989.
16. Multistep Compound Processes in Nuclear Reactions from 9 to 18 MeV. M. B. Chadwick, R. Boretta and P. E. Hodgson, J. Phys. G., 15, 235, 1989.
17. The Neutron Optical Model Potential, P. E. Hodgson, Second Research Co-ordination Meeting to Review Methods for the Calculation of Fast Neutron Nuclear Data for Structural Materials of Fast and Fusion Reactors, Vienna 15-17 February 1988, INDC(NDS)-214/LJ, 49.